Early View

Original research article

Gut microbiota-derived succinate aggravates acute lung injury after intestinal ischemia/reperfusion in mice

Yi-Heng Wang, Zheng-Zheng Yan, Si-Dan Luo, Jing-Juan Hu, Mei Wu, Jin Zhao, Wei-Feng Liu, Cai Li, Ke-Xuan Liu

Gut microbiota-derived succinate aggravates acute lung injury after intestinal ischemia/reperfusion in mice

Yi-Heng Wang[1, 2][#], Zheng-Zheng Yan[1][#], Si-Dan Luo[1], Jing-Juan Hu[1], Mei Wu[1], Jin Zhao[1], Wei-Feng Liu[1], Cai Li[1*], Ke-Xuan Liu[1*]

[1]Department of Anesthesiology, Nanfang Hospital, Southern Medical University, Guangzhou 510515, Guangdong Province, China.
[2]Department of Anesthesiology, The First Affiliated Hospital, Hengyang Medical School, University of South China, Hengyang 421001, Hunan Province, China.

[#] These authors contributed equally.
*Corresponding authors

*Correspondence:

Ke-Xuan Liu, M.D., Ph.D., Cai Li, M.D., Ph.D.

Department of Anesthesiology, Nanfang Hospital, Southern Medical University,

1838 Guangzhou Avenue North,

Guangzhou 510515, China.

Tel: +86-20-87769673;

Email: liukexuan705@163.com (K-X.L.); licaisysu@163.com (C.L.)

Author contributions: K-X.L. and C.L. conceived the project, designed the study, and reviewed and edited the manuscript; Y-H.W. and Z-Z.Y. carried out most of the experiments and prepared the original draft; S-D. L., J-J.H. and J.Z. conducted the

Take home message: Succinate accumulation in the lungs is associated with the imbalance of succinate-producing/-consuming bacteria in the gut during intestinal ischemia/reperfusion. Lung injury was transmissible by gut microbiome, and exacerbated by succinate via alveolar macrophage polarization.

Abstract

Introduction: Acute lung injury (ALI) is a major cause of morbidity and mortality after intestinal ischemia/reperfusion (I/R). Gut microbiota and their metabolic byproducts act as important modulators of the gut–lung axis. This study aimed to define the role of succinate, a key microbiota metabolite, in intestinal I/R-induced ALI progression.

Methods: Gut and lung microbiota of mice subjected to intestinal I/R were analyzed using 16S rRNA gene sequencing. Succinate level alterations were measured in Germ-free (GF) mice or conventional mice treated with antibiotics. Succinate-induced alveolar macrophage polarization and its effects on alveolar epithelial apoptosis were evaluated in succinate receptor1 (*Sucnr1*)-deficient mice and in murine alveolar macrophages transfected with *Sucnr1*-siRNA. Succinate levels were measured in patients undergoing cardiopulmonary bypass, including intestinal I/R.

Results: Succinate accumulated in lungs after intestinal I/R, and this was associated with an imbalance of succinate-producing and succinate-consuming bacteria in the gut, but not the lungs. Succinate accumulation was absent in GF mice and was reversed by gut microbiota depletion with antibiotics, indicating that gut microbiota are a source of lung succinate. Moreover, succinate promoted alveolar macrophage polarization, alveolar epithelial apoptosis, and lung injury during intestinal I/R. Conversely, knockdown of *Sucnr1* or blockage of SUCNR1 *in vitro* and *in vivo* reversed the effects of succinate by modulating PI3K-AKT/HIF-1α pathway. Plasma succinate levels significantly correlated with intestinal I/R-related lung injury after cardiopulmonary bypass.

Conclusion: Gut microbiota-derived succinate exacerbates intestinal I/R–induced ALI through SUCNR1-dependent alveolar macrophage polarization, identifying succinate as a novel target for gut-derived ALI in critically ill patients.

Introduction

Intestinal ischemia/reperfusion (I/R) injury is a fatal condition that frequently occurs after severe traumatic or septic shock, acute mesenteric ischemia, or certain operative procedures, including cardiopulmonary bypass (CPB), small bowel transplantation, and abdominal aortic surgery [1]. Critical injuries occur in the intestinal mucosa and remote organs, resulting in an overall mortality as high as 60–80% [2,3]. Of these remote organ injuries, acute lung injury (ALI) with acute inflammation, increased microvascular permeability, pulmonary edema, and alveolar destruction are the best characterized [4]. Alveolar macrophages (AMs), the most abundant innate immune cells in the airways during lung injury, are the major drivers of lung inflammation [5]. In addition, signals from the microenvironment induce the polarization of AMs to either the pro-inflammatory M1 or anti-inflammatory M2 phenotype [6]. However, the function and modulation of AMs in intestinal I/R-induced ALI have not been fully elucidated.

Gut microbiota and their derived products play a role in a number of pulmonary diseases, including asthma and respiratory infections [7-10], via modulation of innate and adaptive immunity [11, 12]; the link is termed the "gut–lung axis" [13, 14]. Succinate, a classical metabolite of the tricarboxylic acid (TCA) cycle in host cell mitochondria, is an important metabolite of the gut microbiota [15, 16]. Interestingly, not all bacteria produce succinate, some bacteria species are instead succinate-consuming. Succinate levels are regulated by balancing succinate-consuming and -producing bacterial strains [17, 18]. When released into the circulation, gut microbiota-derived succinate acts as a pro-inflammatory signaling molecule in peripheral tissues and plays an essential role in the etiology of

several inflammation-related diseases, such as inflammatory bowel disease, obesity, and type 2 diabetes [17-20]. In a recent study, Riquelme *et al.* found that an excessive amount of succinate was released into the airways during cystic fibrosis and created a microenvironment enhancing susceptibility to infection by *P. aeruginosa*, which is programmed to induce the accumulation of a large variety of metabolites and preferentially catabolize succinate to sustain its growth and long-term colonization of host tissues [21]. Activation of succinate receptor 1 (SUCNR1), a G protein-coupled receptor (GPCR) widely expressed on the plasma membrane of immune cells [22-24], promotes macrophage infiltration and polarization and the release of pro-inflammatory cytokines [23,25]. However, the role of succinate and its receptor SUCNR1 in regulating AMs in the lungs, especially under intestinal I/R conditions, remains largely uncharacterized.

Based on these findings, we hypothesized that intestinal I/R induces an imbalance of succinate-producing and succinate-consuming bacteria in the gut, leading to abundant generation, blood transmission, and succinate accumulation in the lung through the gut–lung axis, subsequently exacerbating lung injury through SUCNR1-dependent AM polarization. The current study evaluated this hypothesis using both animal and human studies in combination with *in vitro* approaches.

Methods

Animal model

A previously described rodent model of intestinal I/R was used [26]. All experimental procedures were performed following the National Institutes of Health Guide for the Care and Use of Laboratory Animals and were approved by the Animal Ethics Committee at Nanfang Hospital, Southern Medical University (Guangdong, China).

One week prior to intestinal I/R, 100 ml succinate (4 or 8 mM/kg per day) or vehicle was injected intraperitoneally. The selected dose and time were based on a previous study [27] and pilot experiments. To deplete the gut microbiota, a cocktail of antibiotics (ABX) (vancomycin, 100 mg/kg; neomycin sulfate, 200 mg/kg; metronidazole, 200 mg/kg; and ampicillin, 200 mg/kg) was suspended in saline and administered to 100 µl/mice via oral gavage once a day for 7 days [28]. See the online supplementary section for further details.

Fecal microbiota transplantation (FMT)

FMT was performed according to a previously described study [29]. Briefly, feces collected from mice (donor mice) under I/R-operation (I/R group) or sham-operation (control group) were resuspended in PBS at 0.125 g/ml. One hundred microliters of the solution were orally administered to Germ-free (GF) mice (receptor mice, 3–6 mice per group) in the corresponding groups via a gastric gavage tube. All mice had free access to food and water, and the gavage was performed in a sterile environment. Three days after transplantation, mice were exposed to intestinal ischemia for 60 min and reperfusion for 4 hours, and then blood, ileum, kidney, lung, and liver samples were harvested sterilely for further examination.

Microbe analysis

The V3–V4 regions of the 16S rRNA gene were amplified and sequenced using an Illumina HiSeq2500 sequencing platform. The raw sequences were first quality-controlled using QIIME (v1.9.1) with default parameters and then demultiplexed and clustered into 50 taxonomic units at the species level (97% similarity). Operational taxonomic unit generation was based on the Greengenes database (v13_8) and the reference-based method from SortMeRNA. Strain composition, alpha diversity, and beta diversity analyses were performed using QIIME (v1.9.1).

Succinate colorimetric assay

Succinate concentrations in the lung tissue, serum, intestine, and cecal contents were determined using a Succinate Colorimetric Assay Kit (BioVision Inc., Milpitas, CA, USA), according to the manufacturer's instructions.

Cell treatment

Primary murine AMs were isolated from C57BL/6J mice [30]. Primary AMs and MH-S cells (a murine AM cell line) were treated with succinate (0.5, 01, 1, 5, or 10 mM) or vehicle for the indicated times. Lipopolysaccharide (100 ng/ml) treatment for 24 h served as a positive control. For some experiments, MH-S cells were pre-treated with specific pharmacological inhibitors (10 µmol/L LY294002 and 100 µmol/L 2-MeOE2) or incubated with anti-SUCNR1/control antibody (IgG) (5 µg/mL) for 1 h prior to stimulation with succinate (1 mM). In addition, a co-culture system was used to detect the effect of

succinate-treated MH-S cells or primary AMs on apoptosis of MLE-12 cells (a murine lung epithelial cell line). Further details are provided in the online supplementary section.

Statistical analysis

All data are expressed as the mean ± SEM. Between-group differences were analyzed with unpaired Student's *t*-test or one-way analysis of variance (ANOVA) followed by *post hoc* Bonferroni's *t*-test. $P < 0.05$ was considered statistically significant. All statistical analyses were performed using SPSS 17.0 (Chicago, IL, USA).

Results

Abnormal accumulation of succinate in the lungs during intestinal I/R was associated with the imbalance of succinate-producing and -consuming bacteria in the gut

Pulmonary succinate levels significantly increased after intestinal I/R and reached a peak (0.58 ± 0.050 mM) at 4 h after reperfusion. This increase was 10.2-fold greater than that in the sham-operated mice. In addition, succinate levels in the cecal contents, intestine, and serum (in order of decreasing concentration) also increased after intestinal I/R in a time-dependent manner (Figure 1A). In addition, a negative correlation was found between pulmonary succinate and mRNA levels of intestinal tight junction-related genes (*Tjp1* and *Ocln*) (Figure 1F-G), indicating that disruption of the mucosal barrier may be associated with succinate accumulation in lung tissue.

16S rRNA gene sequencing of the gut microbiota showed that intestinal I/R led to a significant reduction in the Chao, Shannon diversity, and Simpson indices, which reflected the decreased microbial diversity, richness, and biodiversity at the phylum level (Figure S1A). Comparing the lung microbiota composition, the Chao and Shannon diversity indices were not significantly different between the sham and I/R groups. However, the Simpson index decreased like that of the gut microbiota. The principal component analysis clearly separated the β-diversity of gut and lung samples obtained from I/R- and sham-operated mice (Figure S1A-B). At the family level in the gut microbiota, a significant increase in the *Firmicutes*/*Bacteroidetes* ratio was observed in I/R-treated mice (Figure 1B). Compared to the sham-operated mice, the I/R-treated mice had a higher relative abundance of succinate-producing bacteria at the family (*Prevotellaceae*, *Veillonellaceae*, and *Bacteroidaceae* families) (Figure 1C) and genus levels (*Prevotellaceae UCG-001* and *Paraprevotellaceae spp.*) (Figure 1D). In contrast, the relative abundance of succinate-consuming bacteria was reduced at the family (*Ruminococcaceae*, *Odoribacteraceae,* and *Clostridaceae* families) (Figure 1C) and genus levels (*Ruminococcaceae_1*, *Clostridiaceae_2,* and *Odoribacter spp.*) (Figure 1D). Furthermore, the ratio between specific succinate producers and consumers (*Prevotellaceae* + *Veillonellaceae* + *Bacteroidaceae* / *Ruminococcaceae* + *Odoribacteraceae* + *Clostridaceae*) [Family(P+V+B/R+O+C)] was significantly higher in I/R-treated mice and was positively correlated with pulmonary succinate levels (Figure 1E). No differences were detected in other bacterial families involved in succinate metabolism, such as *Paraprevotellaceae*, *Lachnospiraceae or Rikenellaceae* [31]. In parallel, the bacterial community composition in the lung is very different from that in the

gut at the phylum level. A significant drop in Firmicutes/Bacteroidetes ratio was found in the lung microbiota during intestinal I/R (Figure S1C). Moreover, no significant differences were found in the abundance of succinate-producing and -degrading bacteria in the lung, only accompanied with a significant increase of *Bacteroidaceae* families and a decrease in the abundance of *Carnobacteriaceae* families (Figure S1D). Collectively, intestinal I/R did not affect the balance of succinate-producing and -consuming bacteria in the lung microbiome.

To determine the role of the baseline microbiota differences on biological measurements, we further performed sham- and I/R-operation in mice underwent 7 days singly-housing condition, which could eliminate the possibility of cage effects arising from coprophagy [32,33]. We found that succinate levels significantly increased at 4 h of reperfusion (Figure S2A). 16S rRNA sequencing displayed a reduction in diversity and richness, and an abnormality in the composition at the phylum level in both the gut and lung microbiota. Moreover, an increasing in *Prevotellaceae* families and a decreasing in *Clostridaceae* families were found in the gut microbiota, but not in the lung microbiota of single-housed mice underwent I/R injury (Figure S2B-H). The ratio [Family(P/C)] increased in the I/R-treated mice, and was positively correlated with pulmonary succinate levels (Figure S2E). These results indicate that intestinal I/R treatment itself, rather than the microbiota cage variation, plays a dominant role in the imbalance of succinate-producing and -consuming bacteria in the gut.

The increased amount of pulmonary succinate was derived from gut microbiota

To confirm whether succinate found in the lungs was derived from the gut microbiota, the mice were orally administered a cocktail of broad-spectrum ABX to deplete the gut microbiota (Figure 2A). The results showed that ABX treatment did not affect body weight between the two groups (Figure 2B). Microbiota-depleted mice had significantly reduced succinate levels in the lungs, cecal contents, intestine, and serum at 4 h after reperfusion (Figure 2C). Microbiota-depleted mice also showed less I/R-induced lung injury, based on reduced histopathological scores, total protein concentrations, lung edema (Figure 2D-G), and cytokine levels in the bronchoalveolar lavage fluid (BALF) (Figure 2H). Moreover, we also performed intestinal I/R (60 min/4 h) in GF mice, and the results indicated that succinate levels in the lungs were significantly lower in GF mice than in conventional mice. The declining trend of succinate level was also found in the cecal contents and intestine (Figure 2I).

Intestinal I/R-induced ALI was transmissible by gut microbiome partially via succinate

FMT was performed to demonstrate further that the gut microbiota mediated the phenotype of intestinal I/R-induced ALI and elevation of succinate levels. Recipient mouse lungs were collected on the first and second day after 3 days of FMT (Figure 3A). GF mice that received feces from I/R mice (I/R group) presented a higher level of histopathological scores and cytokines (either in serum or in the lungs) than mice that

received feces from mice under sham operation (control group) (Figure 3B-C). Moreover, a marked increase in lung succinate levels was found in GF mice transplanted with I/R feces compared with those in the control group (Figure 3D). The FMT experiment confirmed that intestinal I/R-induced ALI was transmissible by the gut microbiome, and the mechanism was closely related to gut microbiota byproducts, particularly succinate. In addition, we found that mice treated with FAM-succinate (succinate with FAM-modification) intragastrically presented higher levels of green fluorescence signal intensity in the gut and lung after intestinal I/R (Figure S3A-D), which successfully traced the progression of succinate delivery from the gut to the lung during intestinal I/R. The above results demonstrate that succinate is probably an important mediator of gut microbiota and promotes intestinal I/R-induced ALI through the gut-lung axis.

Succinate induced AM polarization and ALI after intestinal I/R

Mice were treated with succinate (4 and 8 mM/kg/day) or vehicle before intestinal I/R (Figure 4A). Histological analysis of lung tissues revealed the characteristics of ALI. The lung injury severity, lung edema, total protein amount (Figure 4B-C), and cytokine levels in BALF (Figure 4D) were all significantly increased in succinate-treated mice compared with controls, and the effects appeared to be dose-dependent. Succinate also dose-dependently increased the mRNA expression of M1-related markers (*Nos2*, *Ptgs2*, *Ccr7,* and *Tnf*), decreased the expression of M2-related markers (*Arg1*, *Retnla*, *Ccl17,* and *Il10*) (Figure 4E), and increased the number of CD86$^+$CD206$^-$ macrophages in I/R-treated mice (Figure 4F). *In vitro*, gene expression profiling confirmed that succinate

dose-dependently upregulated the expression of M1-related marker genes (*Nos2*, *Ptgs2*, *Ccr7,* and *Tnf*) in primary AMs and MS-H cells (Figure S4A-B).

AMs were essential for the effect of succinate in intestinal I/R-induced ALI

To study the role of AMs in mediating the effects of succinate in intestinal I/R-induced ALI, mice were depleted of AMs by intratracheal injection of liposome-encapsulated clodronate or vehicle (PBS) 72 h before succinate administration (Figure 5A). Successful AM depletion was demonstrated by a notably decreased proportion of F4/80$^+$CD11c$^+$ cells in the BALF (Figure S5A). Clodronate significantly improved histopathological lung injury and reduced alveolar inflammation induced by succinate and intestinal I/R (Figure 5B-F). Co-culture of succinate-polarized MH-S cells with murine lung epithelial cells (MLE-12 cells) increased apoptosis and reduced cell viability among MLE-12 cells (Figure 5H and Figure S5C). Succinate did not display any direct cytotoxic effects on MLE-12 cells (Figure 5G and Figure S5B).

Succinate promoted AM polarization and ALI via SUCNR1 after intestinal I/R

Immunofluorescence revealed the colocalization of SUCNR1-positive cells with resident AMs in and around the alveolar interstitium. The proportion of SUCNR1-positive cells expressing the AM marker F4/80 markedly increased in the lungs of succinate-treated mice underwent intestinal I/R (Figure 6A-B). Moreover, the protein and mRNA expression levels of SUCNR1 in AM pellets were significantly increased after intestinal I/R and further enhanced after succinate treatment (Figure 6C-D).

Sucnr1^{-/-} and wild-type (WT) mice were treated with succinate for 1 week before intestinal I/R. *Sucnr1^{-/-}* mice displayed a significantly lower degree of lung injury based on histopathology (Figure 6E), pulmonary inflammation (Figure S6A), M1-related marker mRNA expression (Figure 6F), and the proportion of CD86$^+$CD206$^-$ AMs (Figure 6I and Figure S6C) compared to WT mice following succinate treatment. In addition, an *in vivo* neutralization assay of antibody against SUCNR1 (2.5 μg/g, intravenously) was performed in WT mice. The results revealed that lung injuries, including lung histology scores (Figure 6G), BALF protein levels, the degree of lung edema and pulmonary inflammation (Figure S6B) was significantly blocked with anti-SUCNR1 antibody. *In vitro,* the succinate-induced M1 polarization of MH-S treated with neutralizing antibody of SUCNR1 (anti-SUCNR1, 5 μg/ml) (anti-SUCNR1+ Succinate group) was significantly inhibited compared with the IgG+ Succinate group (Figure 6H).

The number of terminal deoxynucleotidyl transferase dUTP nick end labeling (TUNEL)-positive cells was significantly lower in the lungs of *Sucnr1^{-/-}* mice than that in WT mice (Figure 6J and Figure S6E). *In vitro, Sucnr1* absence completely suppressed MLE-12 cell apoptosis caused by co-culture with succinate-polarised AMs (Figure 6K and Figure S6D).

The PI3K/AKT/HIF-1α pathway participated in succinate-induced AM polarization and ALI after intestinal I/R.

Considering the crucial role of PI3K/AKT/HIF-1α signaling in macrophage activation, metabolism, and polarization[34], the roles of these signaling molecules in mediating the effects of succinate were investigated. Succinate induced phosphorylation of AKT and upregulation of HIF-1α in I/R-treated WT mice (Figure 7A-B) and succinate-treated MH-S cells (Figure 7C-E). However, this upregulation was absent in $Sucnr1^{-/-}$ mice and MH-S cells transfected with $Sucnr1$-siRNA (Figure 7A–E).

Succinate-induced polarized MH-S cells were treated with specific pharmacological inhibitors of HIF-1α (2-MeOE2) and PI3K (LY294002), separately. Both 2-MeOE2 and LY294002 suppressed succinate-induced upregulation of M1-related markers in MH-S cells (Figure 7F) and succinate-polarized AM-induced apoptosis in MLE-12 cells (Figure 7I and Figure S7A-B). Inhibition of the PI3K/AKT pathway also abrogated succinate-induced expression of HIF-1α at protein (Figure 7G) and mRNA (Figure 7H) levels.

Plasma succinate levels correlated with intestinal I/R-related lung injury after cardiopulmonary bypass in patients.

Intestinal I/R is a critical event and a leading risk factor for remote organ injury during cardiac surgery with CPB [35]. Plasma succinate levels increased significantly 1 h after CPB and returned to baseline levels 24 h after CPB (Figure S8A). Elevated succinate levels (1 h after CPB) were significantly correlated with impaired lung function, as

reflected by a reduced PaO_2/FiO_2 ratio and prolonged mechanical ventilation time (Figure S8B-C). Moreover, elevated succinate levels were positively correlated with the pulmonary surfactant D (SP-D) and TNF-α concentrations, which partly reflected alveolar damage and inflammation, respectively (Figure S8D-E). The clinical characteristics of the study participants are presented in Table S1.

Discussion

This study is the first to establish the role of gut microbiota-derived succinate in the development of intestinal I/R-induced ALI. We identified abnormal pulmonary succinate accumulation and its close relationship with the imbalance of certain succinate-producing/consuming bacteria. Succinate accumulation was absent in GF mice and reversed by microbiota depletion with ABX oral administration in conventional mice, indicating that the gut microbiota are a source of succinate. The exacerbation of I/R-induced ALI by succinate was partially mediated by the succinate receptor SUCNR1 and its interference with AM polarization. This was demonstrated by the results showing that the detrimental effects of succinate were abrogated in AM-depleted mice, SUCNR1 blockage mice, $Sucnr1^{-/-}$ mice, and a murine AM cell line with siRNA-induced $Sucnr1$ knockdown. Mechanistically, the PI3K/AKT/HIF-1α signaling involvement was verified *in vivo* and *in vitro*. In humans, elevated plasma succinate levels were associated with lung injury in patients undergoing CPB including intestinal I/R injury. Together, these data indicate that gut microbiota-derived succinate promotes AM polarization and aggravates ALI after intestinal I/R and that the SUCNR1 receptor and PI3K/AKT/HIF-1α signaling pathways participate in this process.

Succinate accumulation is a common metabolic event in I/R, cancer, and obesity [36,37]. Here in this study, succinate abnormally accumulated in the cecal contents, intestinal, plasma, and lung after intestinal I/R, which responsible for the subsequent lung injury. Interestingly, it was reported that specific diets (such as high-fat diets, high-fiber diets and elemental diets, *etc*) affect succinate levels and gut microbiota composition [38,39]. These studies open a new window for the exploration of the therapeutic potential of various dietary interventions in intestinal I/R induced lung injury. In addition, we found that pulmonary succinate accumulation correlated with the ratio of gut succinate-producing/consuming bacteria and was accompanied by the disruption of intestinal mucosal integrity. Our results suggest that similar to that seen in obese patients and colitis mice [17,18], an imbalance between the families of intestinal bacteria classified as succinate-producers (*Prevotellaceae*, *Veillonellaceae*, and *Bacteroidaceae*) and succinate-consumers (*Ruminococcaceae*, *Odoribacteraceae*, and *Clostridaceae*) was discovered in the gut. However, the composition of succinate-producing/consuming bacteria was not significantly different between the groups in the lungs, indicating accumulated succinate in the lungs was possibly derived from gut microbiota. We also found that when oral administration with FAM fluorophore-conjugated succinate, the green fluorescence intensity increased in the intestine and the lungs of I/R-challenged mice (Figure S3C-D), indicating that the accumulated succinate in the lungs was, at least in part, originated from the intestine that subsquently delivering through the gut-lung axis. Consistent with this, gut microbiota depletion under ABX or germ-free conditions abrogated pulmonary succinate accumulation during intestinal I/R (Figure 2C and I); Meanwhile, fecal microbiota transplantation on GF mice with feces of I/R mice increased

lung succinate levels (Figure 3D). All the evidence suggests that succinate is likely produced by the gut microbiota and acts as an important mediator of the gut–lung axis during intestinal I/R.

Lung microbiota also plays a key role in lung immunity during inflammation. It was reported that the variation in lung microbiota is associated with pulmonary inflammation and injury, and is predictive of disease progression and clinical outcomes [40,41]. The diversity and community composition of lung microbiota are correlated with alveolar inflammation indices; Meanwhile, the absence of microbiota in GF mice protects against mortality in the fibrotic lung [42]. In our study, 16S rRNA sequencing of lung microbiota revealed that there were significant drops in Simpson index and Firmicutes/Bacteroidetes ratio after I/R treatment. The lung microbiota changes may contribute to lung inflammation and injuries during intestinal I/R.

We also found that succinate polarizes AMs towards the pro-inflammatory M1 phenotype during intestinal I/R. AMs are highly specialized tissue-resident macrophages that colonize the respiratory surface of the lungs and have the unique ability to dynamically adapt to the local microenvironment via polarization into pro-inflammatory M1 or anti-inflammatory M2 phenotypes [5, 6]. In this study, succinate treatment increased the expression of M1 marker genes (*Nos2*, *Ptgs2*, *Ccr7,* and *Tnf*) and CD86$^+$CD206$^-$-AM population after intestinal I/R. AM depletion completely inhibited succinate-induced

inflammation and ALI, suggesting a crucial role of polarized AMs in mediating the effects of succinate. This is further supported by our *in vitro* experiments, which showed that exogenous succinate augmented the expression of M1 marker genes in MH-S cells and primary AMs.

We further prove that the succinate receptor SUCNR1 is crucial for succinate-induced AM polarization. SUCNR1 is expressed on the membranes of resident macrophages in the intestine, adipose tissue, and lung tumors [23, 25, 37]. A recent study showed that upregulation and activation of SUCNR1 on intestinal macrophages increases the expression of pro-inflammatory cytokines and M1 marker genes in intestinal and peritoneal macrophages, while *Sucnr1* deficiency shifts the macrophages towards the M2 phenotype, thus protecting mice from colitis [23]. However, literature findings are not unanimous. Another study demonstrated that SUCNR1 activation promotes polarization towards the anti-inflammatory M2 phenotype in adipose tissue-resident macrophages and increases the response to type 2 cytokines, including IL-4 [43]. Therefore, different macrophages may respond differently to SUCNR1 activation. In the present study, succinate treatment during intestinal I/R enhanced SUCNR1 expression on AMs. SUCNR1 activation promotes M1-polarization, amplifies lung inflammation, and leads to ALI. In contrast, *Sucnr1* deficiency or utilization of a SUCNR1 neutralizing antibody suppressed succinate-induced AM polarization and/or ALI. Hence, we concluded that the effect of succinate on AM polarization during intestinal I/R is, at least in part, mediated by the activation of SUCNR1 on AMs.

The current study also demonstrates the important role of HIF-1α in succinate-enhanced intestinal I/R-induced ALI. Previous studies have shown that a sustained increase in succinate induces the pro-inflammatory cytokine IL-1β via HIF-1α [44] and triggers tumor-associated macrophage polarization via PI3K/AKT/HIF-1α signaling [35]. In this study, a selective HIF-1α inhibitor abrogated succinate-induced AM polarization, suggesting that HIF-1α activation is essential for this process. HIF-1α activates the transcription of hypoxia-response genes, and HIF-1α inhibition has been associated with regulating macrophage polarization by preventing anaerobic glycolysis involved in glucose metabolism reprogramming [45]. Furthermore, we found that pharmacological inhibitors of PI3K inhibited HIF-1α expression, and subsequent AM polarization and alveolar epithelial cell apoptosis, suggesting that PI3K plays an important role in regulating HIF-1α activation. However, like most GPCRs, SUCNR1 can activate multiple signaling pathways in a cell-specific manner [46]. The exact signaling pathway and functions of SUCNR1 require further research.

In addition, we observed increased plasma succinate levels after CPB, a procedure associated with intestinal I/R. The over-release of succinate into circulation is likely common during CPB, and intestinal I/R may participate in this process. Our study further showed that succinate is particularly relevant to lung function impairment, alveolar damage, and pulmonary inflammation. Therefore, succinate may represent a novel circulating biomarker of intestinal I/R-related ALI during CPB.

This study has several limitations. First, excessive succinate may originate from dying epithelial cells and glutamine-dependent anaplerosis in host cells [47]. Further studies are warranted to investigate these host-derived sources of succinate. Second, although the microbiota of mice was normalized by co-housing, there still have baseline difference of microbiota in individual mice, which is a source of confounder in this microbial study [32, 33]. Third, succinate levels were only assessed in patients' peripheral blood and not in fecal samples because of the difficulty in collecting fecal samples from patients with reduced intestinal peristalsis after cardiac surgery. Succinate levels should be determined in fecal samples and blood, and gut microbiota characteristics should be examined. Finally, further investigations are required to define the role of other microbiome mediators (short-chain fatty acid, tryptophan metabolites, *etc.*), both remotely from the gut and locally from within the respiratory tract, in the development of ALI.

In summary, we have shown that gut microbiota are the source of elevated succinate in the lungs during intestinal I/R. Moreover, succinate exacerbates intestinal I/R-induced ALI by modulating AM polarization. We also provide evidence that succinate exerts its effects, at least partially, via the SUCNR1 and the PI3K/AKT/HIF-1α pathways (Figure 8). These findings identified succinate as a microbiota metabolite that may be a valuable target for the treatment of gut-derived ALI in critically ill patients.

References

1.Tendler DA. Acute intestinal ischemia and infarction. Semin Gastrointest Dis 2003: 14(2): 66-76.

2.Gonzalez LM, Moeser AJ, Blikslager AT. Animal models of ischemia-reperfusion-induced intestinal injury: progress and promise for translational research. *Am J Physiol Gastrointest Liver Physiol* 2015: 308(2): G63-75.

3.Matthay MA, Zimmerman GA, Esmon C, Bhattacharya J, Coller B, Doerschuk CM, Floros J, Gimbrone MA, Jr., Hoffman E, Hubmayr RD, Leppert M, Matalon S, Munford R, Parsons P, Slutsky AS, Tracey KJ, Ward P, Gail DB, Harabin AL. Future research directions in acute lung injury: summary of a National Heart, Lung, and Blood Institute working group. *Am J Respir Crit Care Med* 2003: 167(7): 1027-1035.

4.   Matthay MA, Ware LB, Zimmerman GA. The acute respiratory distress syndrome. *The Journal of clinical investigation* 2012: 122(8): 2731-2740.

5.   Huang X, Xiu H, Zhang S, Zhang G. The Role of Macrophages in the Pathogenesis of ALI/ARDS. *Mediators of inflammation* 2018: 2018: 1264913.

6.   Johnston LK, Rims CR, Gill SE, McGuire JK, Manicone AM. Pulmonary macrophage subpopulations in the induction and resolution of acute lung injury. *American journal of respiratory cell and molecular biology* 2012: 47(4): 417-426.

7.   Barcik W, Boutin RCT, Sokolowska M, Finlay BB. The Role of Lung and Gut Microbiota in the Pathology of Asthma. *Immunity* 2020: 52(2): 241-255.

8.   Schuijt TJ, Lankelma JM, Scicluna BP, de Sousa e Melo F, Roelofs JJ, de Boer JD, Hoogendijk AJ, de Beer R, de Vos A, Belzer C, de Vos WM, van der Poll T, Wiersinga WJ. The gut microbiota plays a protective role in the host defence against pneumococcal pneumonia. *Gut* 2016: 65(4): 575-583.

9. Coffey MJ, Nielsen S, Wemheuer B, Kaakoush NO, Garg M, Needham B, Pickford R, Jaffe A, Thomas T, Ooi CY. Gut Microbiota in Children With Cystic Fibrosis: A Taxonomic and Functional Dysbiosis. *Scientific reports* 2019: 9(1): 18593.

10. Kapur R, Kim M, Rebetz J, Hallström B, Björkman JT, Takabe-French A, Kim N, Liu J, Shanmugabhavananthan S, Milosevic S, McVey MJ, Speck ER, Semple JW. Gastrointestinal microbiota contributes to the development of murine transfusion-related acute lung injury. *Blood advances* 2018: 2(13): 1651-1663.

11. Budden KF, Gellatly SL, Wood DL, Cooper MA, Morrison M, Hugenholtz P, Hansbro PM. Emerging pathogenic links between microbiota and the gut-lung axis. *Nature reviews Microbiology* 2017: 15(1): 55-63.

12. Krzyzaniak MJ, Peterson CY, Cheadle G, Loomis W, Wolf P, Kennedy V, Putnam JG, Bansal V, Eliceiri B, Baird A, Coimbra R. Efferent vagal nerve stimulation attenuates acute lung injury following burn: The importance of the gut-lung axis. *Surgery* 2011: 150(3): 379-389.

13. Dang AT, Marsland BJ. Microbes, metabolites, and the gut-lung axis. *Mucosal immunology* 2019: 12(4): 843-850.

14. Wypych TP, Wickramasinghe LC, Marsland BJ. The influence of the microbiome on respiratory health. *Nature immunology* 2019: 20(10): 1279-1290.

15. Connors J, Dawe N, Van Limbergen J. The Role of Succinate in the Regulation of Intestinal Inflammation. *Nutrients* 2018: 11(1).

16. Faith JJ, Ahern PP, Ridaura VK, Cheng J, Gordon JI. Identifying gut microbe-host phenotype relationships using combinatorial communities in gnotobiotic mice. *Science translational medicine* 2014: 6(220): 220ra211.

17. Serena C, Ceperuelo-Mallafré V, Keiran N, Queipo-Ortuño MI, Bernal R, Gomez-Huelgas R, Urpi-Sarda M, Sabater M, Pérez-Brocal V, Andrés-Lacueva C, Moya A, Tinahones FJ, Fernández-Real JM, Vendrell J, Fernández-Veledo S. Elevated circulating levels of succinate in human obesity are linked to specific gut microbiota. *The ISME journal* 2018: 12(7): 1642-1657.

18. Ariake K, Ohkusa T, Sakurazawa T, Kumagai J, Eishi Y, Hoshi S, Yajima T. Roles of mucosal bacteria and succinic acid in colitis caused by dextran sulfate sodium in mice. *Journal of medical and dental sciences* 2000: 47(4): 233-241.

19. de Vadder F, Mithieux G. Gut-brain signaling in energy homeostasis: the unexpected role of microbiota-derived succinate. *The Journal of endocrinology* 2018: 236(2):

R105-r108.

20. Mills E, O'Neill LA. Succinate: a metabolic signal in inflammation. *Trends in cell biology* 2014: 24(5): 313-320.

21. Riquelme SA, Lozano C, Moustafa AM, Liimatta K, Tomlinson KL, Britto C, Khanal S, Gill SK, Narechania A, Azcona-Gutiérrez JM, DiMango E, Saénz Y, Planet P, Prince A. CFTR-PTEN-dependent mitochondrial metabolic dysfunction promotes *Pseudomonas aeruginosa* airway infection. *Sci Transl Med* 2019: 11(499):eaav4634.

22. Rubic T, Lametschwandtner G, Jost S, Hinteregger S, Kund J, Carballido-Perrig N, Schwärzler C, Junt T, Voshol H, Meingassner JG, Mao X, Werner G, Rot A, Carballido JM. Triggering the succinate receptor GPR91 on dendritic cells enhances immunity. *Nature immunology* 2008: 9(11): 1261-1269.

23. Macias-Ceja DC, Ortiz-Masiá D, Salvador P, Gisbert-Ferrándiz L, Hernández C, Hausmann M, Rogler G, Esplugues JV, Hinojosa J, Alós R, Navarro F, Cosin-Roger J, Calatayud S, Barrachina MD. Succinate receptor mediates intestinal inflammation and fibrosis. *Mucosal immunology* 2019: 12(1): 178-187.

24. Littlewood-Evans A, Sarret S, Apfel V, Loesle P, Dawson J, Zhang J, Muller A, Tigani B, Kneuer R, Patel S, Valeaux S, Gommermann N, Rubic-Schneider T, Junt T, Carballido JM. GPR91 senses extracellular succinate released from inflammatory macrophages and exacerbates rheumatoid arthritis. *The Journal of experimental medicine* 2016: 213(9): 1655-1662.

25. van Diepen JA, Robben JH, Hooiveld GJ, Carmone C, Alsady M, Boutens L, Bekkenkamp-Grovenstein M, Hijmans A, Engelke UFH, Wevers RA, Netea MG, Tack CJ, Stienstra R, Deen PMT. SUCNR1-mediated chemotaxis of macrophages aggravates

obesity-induced inflammation and diabetes. *Diabetologia* 2017: 60(7): 1304-1313.

26. Zhang XY, Liang HS, Hu JJ, Wan YT, Zhao J, Liang GT, Luo YH, Liang HX, Guo XQ, Li C, Liu WF, Liu KX. Ribonuclease attenuates acute intestinal injury induced by intestinal ischemia reperfusion in mice. *International immunopharmacology* 2020: 83: 106430.

27. Guo Y, Xie C, Li X, Yang J, Yu T, Zhang R, Zhang T, Saxena D, Snyder M, Wu Y, Li X. Succinate and its G-protein-coupled receptor stimulates osteoclastogenesis. Nature communications 2017: 8: 15621.

28. Gong S, Yan Z, Liu Z, Niu M, Fang H, Li N, Huang C, Li L, Chen G, Luo H, Chen X, Zhou H, Hu J, Yang W, Huang Q, Schnabl B, Chang P, Billiar TR, Jiang Y, Chen P. Intestinal Microbiota Mediates the Susceptibility to Polymicrobial Sepsis-Induced Liver Injury by Granisetron Generation in Mice. Hepatology (Baltimore, Md) 2019: 69(4): 1751-1767.

29. Hu J, Deng F, Zhao B, Lin Z, Sun Q, Yang X, Wu M, Qiu S, Chen Y, Yan Z, Luo S, Zhao J, Liu W, Li C, Liu KX. Lactobacillus murinus alleviate intestinal ischemia/reperfusion injury through promoting the release of interleukin-10 from M2 macrophages via Toll-like receptor 2 signaling. Microbiome 2022: 10(1): 38.

30. Janssen WJ, McPhillips KA, Dickinson MG, Linderman DJ, Morimoto K, Xiao YQ, Oldham KM, Vandivier RW, Henson PM, Gardai SJ. Surfactant proteins A and D suppress alveolar macrophage phagocytosis via interaction with SIRP alpha. *Am J Respir Crit Care Med* 2008: 178(2): 158-167.

31. Fernández-Veledo S, Vendrell J. Gut microbiota-derived succinate: Friend or foe in human metabolic diseases? *Reviews in endocrine & metabolic disorders* 2019: 20(4):

439-447.

32. Witjes VM, Boleij A, Halffman W. Reducing versus Embracing Variation as Strategies for Reproducibility: The Microbiome of Laboratory Mice. *Animals (Basel)* 2020:10(12):2415.

33. Russell A, Copio JN, Shi Y, Kang S, Franklin CL, Ericsson AC. Reduced housing density improves statistical power of murine gut microbiota studies. *Cell Rep* 2022:39(6):110783.

34. Sica A, Mantovani A. Macrophage plasticity and polarization: in vivo veritas. *The Journal of clinical investigation* 2012: 122(3): 787-795.

35. Adamik B, Kübler A, Gozdzik A, Gozdzik W. Prolonged Cardiopulmonary Bypass is a Risk Factor for Intestinal Ischaemic Damage and Endotoxaemia. *Heart, lung & circulation* 2017: 26(7): 717-723.

36. Chouchani ET, Pell VR, Gaude E, Aksentijević D, Sundier SY, Robb EL, Logan A, Nadtochiy SM, Ord ENJ, Smith AC, Eyassu F, Shirley R, Hu CH, Dare AJ, James AM, Rogatti S, Hartley RC, Eaton S, Costa ASH, Brookes PS, Davidson SM, Duchen MR, Saeb-Parsy K, Shattock MJ, Robinson AJ, Work LM, Frezza C, Krieg T, Murphy MP. Ischaemic accumulation of succinate controls reperfusion injury through mitochondrial ROS. *Nature* 2014; 515: 431-435.

37. Wu JY, Huang TW, Hsieh YT, Wang YF, Yen CC, Lee GL, Yeh CC, Peng YJ, Kuo YY, Wen HT, Lin HC, Hsiao CW, Wu KK, Kung HJ, Hsu YJ, Kuo CC. Cancer-Derived Succinate Promotes Macrophage Polarization and Cancer Metastasis via Succinate Receptor. Molecular cell 2020: 77(2): 213-227.e215.

38. Jakobsdottir G, Xu J, Molin G, Ahrné S, Nyman M. High-fat diet reduces the

formation of butyrate, but increases succinate, inflammation, liver fat and cholesterol in rats, while dietary fibre counteracts these effects. *PLoS One* 2013:8(11):e80476.

39. Kajiura T, Takeda T, Sakata S, Sakamoto M, Hashimoto M, Suzuki H, Suzuki M, Benno Y.Change of intestinal microbiota with elemental diet and its impact on therapeutic effects in a murine model of chronic colitis. *Dig Dis Sci* 2009:54(9):1892-900

40. Panzer AR, Lynch SV, Langelier C, Christie JD, McCauley K, Nelson M, Cheung CK, Benowitz NL, Cohen MJ, Calfee CS. Lung Microbiota Is Related to Smoking Status and to Development of Acute Respiratory Distress Syndrome in Critically Ill Trauma Patients. *Am J Respir Crit Care Med* 2018:197(5):621-631.

41.Dickson RP, Singer BH, Newstead MW, Falkowski NR, Erb-Downward JR, Standiford TJ, Huffnagle GB. Enrichment of the lung microbiome with gut bacteria in sepsis and the acute respiratory distress syndrome. *Nat Microbiol* 18;1(10):16113.

42. O'Dwyer DN, Ashley SL, Gurczynski SJ, Xia M, Wilke C, Falkowski NR, Norman KC, Arnold KB, Huffnagle GB, Salisbury ML, Han MK, Flaherty KR, White ES, Martinez FJ, Erb-Downward JR, Murray S, Moore BB, Dickson RP. Lung Microbiota Contribute to Pulmonary Inflammation and Disease Progression in Pulmonary Fibrosis. *Am J Respir Crit Care Med* 2019: 199(9):1127-1138.

43. Keiran N, Ceperuelo-Mallafré V, Calvo E, Hernández-Alvarez MI, Ejarque M, Núñez-Roa C, Horrillo D, Maymó-Masip E, Rodríguez MM, Fradera R, de la Rosa JV, Jorba R, Megia A, Zorzano A, Medina-Gómez G, Serena C, Castrillo A, Vendrell J, Fernández-Veledo S. SUCNR1 controls an anti-inflammatory program in macrophages to regulate the metabolic response to obesity. *Nat Immunol* 2019; 20: 581-592.

44. Tannahill GM, Curtis AM, Adamik J, Palsson-McDermott EM, McGettrick AF, Goel G,

Frezza C, Bernard NJ, Kelly B, Foley NH, Zheng L, Gardet A, Tong Z, Jany SS, Corr SC, Haneklaus M, Caffrey BE, Pierce K, Walmsley S, Beasley FC, Cummins E, Nizet V, Whyte M, Taylor CT, Lin H, Masters SL, Gottlieb E, Kelly VP, Clish C, Auron PE, Xavier RJ, O'Neill LA. Succinate is an inflammatory signal that induces IL-1β through HIF-1α. *Nature* 2013: 496(7444): 238-242.

45. Wang T, Liu H, Lian G, Zhang SY, Wang X, Jiang C. HIF1α-Induced Glycolysis Metabolism Is Essential to the Activation of Inflammatory Macrophages. *Mediators of inflammation* 2017: 2017: 9029327.

46. Gilissen J, Jouret F, Pirotte B, Hanson J. Insight into SUCNR1 (GPR91) structure and function. *Pharmacology & therapeutics* 2016: 159: 56-65.

47. Slaughter AL, D'Alessandro A, Moore EE, Banerjee A, Silliman CC, Hansen KC, Reisz JA, Fragoso M, Wither MJ, Bacon AW, Moore HB, Peltz ED. Glutamine metabolism drives succinate accumulation in plasma and the lung during hemorrhagic shock. *The journal of trauma and acute care surgery* 2016: 81(6): 1012-1019.

Figures and legends:

Figure 1: Elevated lung succinate was associated with dysbiosis and specific changes in gut microbiota related to succinate metabolism during intestinal I/R.
(A) The succinate levels increased in the lung, cecal contents, intestine and serum after 1, 2, 4, 6, or 8 h of reperfusion. **(B)** Microbiota composition at phylum levels was altered, and the Firmicutes/Bacteroidetes ratio was increased during intestinal I/R. **(C)** Intestinal I/R lead to increases in succinate-producing species *(Prevotellaceae, Tannerellaceae,* and *Bacteroidacea*) and decreases in succinate-consuming species (*Ruminococcaceae, Clostridiaceae,* and *Odoribacteraceae*). **(D)** At the genus level, there was an increase in the abundance of succinate-producing strains (*Prevotellaceae UCG-001* and *Paraprevotellaceae spp.*) and a decrease in the abundance of succinate-consuming strains (*Ruminococcaceae_1, Clostridiaceae_2,* and *Odoribacter spp.*). **(E)** The pulmonary succinate level was positively correlated with the ratio between succinate producers (*Prevotellaceae+ Tannerellaceae+Bacteroidacea, P+T+B*) and succinate consumers (*Ruminococcaceae+Odoribacteraceae+Clostridiaceae, R+O+C*) [(P+T+B)/(R+O+C) ratio]. **(F-G)** The pulmonary succinate level was negatively correlated with the mRNA levels of mucosa tight junction genes *Tjp1* and *Ocln.* Data are expressed as mean ± SEM. (A) n = 6–8; (B–G) n = 10. $^{*}P$ < 0.05, $^{**}P$ < 0.01, $^{***}P$ < 0.001 vs. sham group.

Figure 2: Elevated pulmonary succinate levels and intestinal I/R-induced lung injury were reversed after gut microbiota depletion.
(A) Conventional mice, pseudo sterile mice depleted gut microbiota with antibiotics (ABX) and Germ-free (GF) mice underwent sham- and I/R-operation, and succinate levels and/or the degree of lung injury were measured. **(B)** ABX treatment has no effect on body weight compared with PBS group (n = 6). **(C)** ABX treatment reversed succinate increase in the lung, serum, cecal contents and intestine (n = 6). **(D)** Representative H&E staining images (bar = 100 μm). **(E-H)** The increases in histological scores, lung water contents, protein contents of BALF and pro-inflammatory cytokines (TNF-α, IL-1β and

IL-6) were reversed after ABX treatment (n = 6). **(I)** Succinate level presented lower in GF mice than that in conventional (CV) mice, either under sham-or I/R-operation (n = 3). Data are expressed as mean ± SEM. [**]P < 0.01, [***]P < 0.001, versus sham group; [#]P < 0.05, [##]P < 0.01, [###]P < 0.001, vs. I/R group.

Figure 3: Transplantation with fecal microbiota of conventional I/R mice to GF mice significantly aggravates lung injury and succinate accumulation. (A) Germ-free (GF) mice were transplanted with the feces collected from conventional mice that underwent a sham-operation (control group) and I/R-operation (I/R group) intragastrically for 3 days, and the degree of lung injury and levels of succinate were evaluated. **(B-C)** GF mice in the I/R group presented a higher level of histopathological scores (bar = 200 μm) (B) and pro-inflammatory cytokines in serum or the lung (C) than GF mice in the control group (n = 6). **(E)** Succinate levels were significantly increased in GF mice in the I/R group compared with those in the control group (n = 6). Data are expressed as mean ± SEM. [*]P < 0.05, [**]P < 0.01, [***]P < 0.001, vs. control 24 h group; [#]P < 0.05, vs. control 48 h group.

Figure 4: Succinate polarized AM towards M1 phenotype and aggravated lung injury after intestinal I/R. (A) C57BL/6J mice received intraperitoneal (i.p.) injection of 4 or 8 mM/kg/d succinate for 7 days before intestinal I/R. **(B-E)** Succinate dose-dependently promoted lung histological damage as seen on H&E staining (bar = 200 μm) (n = 6), (B) and inflammation as demonstrated by histological score, lung water contents, and the levels of BALF protein (C) and pro-inflammatory cytokines (D) after intestinal I/R (n = 6). **(E)** Succinate enhanced the expression of M1-related genes (*Nos2, Ptgs2, Ccr7,* and *Tnf*) while inhibiting the expression of M2-related genes (*Arg1, Retnla, Ccl17,* and *Il10*) (n = 6). **(F)** Succinate increased the population of CD86^{+}CD206^{-} M1 macrophages, while reducing the numbers of CD86^{-}CD206^{+} M2 macrophages (n = 3). Data are expressed as mean ± SEM. [*]P < 0.05, [**]P < 0.01, [***]P < 0.001, vs. PBS-alone group; [#]P < 0.05, [##]P < 0.01, [###]P < 0.001, vs. I/R-alone group.

Figure 5: Activation of AMs was essential for succinate-mediated lung injury during intestinal I/R. (A) To deplete AMs, succinate-injected mice received intratracheal (i.t.) injection with liposome-encapsulated clodronate 3 days prior to i.p. injection of 8 mM/kg/d succinate. Control mice were injected with liposome-encapsulated PBS. The AM depletion efficiency was analyzed by flow cytometry. **(B-F)** Depletion alleviated succinate-induced lung damage and inflammation after intestinal I/R, as seen by H&E staining (B) and histological score (bar = 200 μm), lung water contents (D), the levels of BALF protein (E), and BALF pro-inflammatory cytokines (F) ($n = 6$). Data are expressed as mean ± SEM. $^*P < 0.05$, $^{**}P < 0.01$, $^{***}P < 0.001$, vs. vehicle group; $^\#P < 0.05$, $^{\#\#}P < 0.01$, $^{\#\#\#}P < 0.001$, vs. vehicle+succinate group. **(G-H)** Succinate had no direct effect on cell viability and apoptosis of MLE-12 cells, whereas co-culture with succinate-induced polarized MH-S cells promoted MLE-12 cell apoptosis ($n = 3$) and reduced cell viability ($n = 6$). Data are expressed as mean ± SEM. $^{***}P < 0.001$, vs. monoculture group.

Figure 6: SUCNR1 signaling mediated succinate-induced AM polarization and lung injury after intestinal I/R. WT and *Sucnr1$^{-/-}$* mice received intraperitoneal (i.p.) succinate injection (8 mM/kg/d) for 7 days before intestinal I/R. **(A-D)** The expression of SUCNR1 on AMs was upregulated after succinate treatment. Succinate induced increases in the *Sucnr1*$^+$F4/80$^+$ cell population (A and B, arrows indicate the colocalization of SUCNR1 and F4/80, bar = 50 μm) ($n = 3$), and the levels of *Sucnr1* mRNA (C) ($n = 3$) and protein (D) ($n = 6$) in AMs. Data are expressed as mean ± SEM. $^*P < 0.05$, $^{**}P < 0.01$, $^{***}P < 0.001$, vs. control group; $^{\#\#}P < 0.01$, vs. succinate group. **(E)** *Sucnr1* deficiency attenuated succinate-induced lung injury as observed by H&E staining (bar = 200 μm ($n = 6$). **(F)** *Sucnr1* deficiency eliminated the succinate-induced upregulation of M1-related genes (n = 6). **(G)** Anti-SUCNR1 antibody reduced lung injury in mice, as seen by H&E staining (bar = 200 μm) ($n = 3$). Data are expressed as mean ± SEM. *$P < 0.05$, vs. PBS group; $^\#P < 0.05$, vs. IgG group. **(H)** MH-S incubated with anti-SUCNR1 inhibited the succinate-induced upregulation of M1-related genes ($n = 6$). Data are expressed as mean ± SEM. $^{***}P < 0.001$, vs. control group; $^{\#\#}P < 0.01$, $^{\#\#\#}P < 0.001$, vs. IgG+succinate group. **(I)** *Sucnr1* deficiency increase the percentage of

CD86$^+$CD206$^-$ M1-macrophages during intestinal I/R (n = 3). **(J)** *Sucnr1* deficiency suppressed succinate-induced cell apoptosis in the lung during intestinal I/R (n = 3). (F, H, I) Data are expressed as mean ± SEM. $^*P$ < 0.05, $^{**}P$ < 0.01, $^{***}P$ < 0.001, vs. WT mice I/R group; $^{##}P$ < 0.01, $^{###}P$ < 0.001, vs. WT mice with succinate+I/R group. **(K)** *In vitro*, *Sucnr1* deletion completely abolished succinate-induced apoptosis of MLE-12 cells co-cultured with polarized AMs (n = 3). Data are expressed as mean ± SEM. $^*P$ < 0.05, $^{***}P$ < 0.001, vs. WT mice PBS-treated group; $^{###}P$ < 0.001, vs. WT mice succinate-treated group.

Figure 7: PI3K/AKT/HIF-1α signaling was required for succinate-induced AM polarization and lung injury following intestinal I/R. (A-B) The activation of HIF-1α and phosphorylation of AKT were enhanced upon succinate treatment, while these effects were reversed by *Sucnr1* deficiency in *Sucnr1*$^{-/-}$ mice during intestinal I/R injury (A,n = 3; B,n = 6). Data are expressed as mean ± SEM. $^*P$ < 0.05, $^{**}P$ < 0.01, $^{***}P$ < 0.001, vs.WT mice I/R group; $^{##}P$ < 0.01, $^{###}P$ < 0.001, vs. WT mice with succinate+I/R group. **(C-E)** The upregulation of SUCNR1, HIF-1α and phosphorylation of AKT was absent in *Sucnr1*$^{-/-}$ mice and MH-S cells transfected with *Sucnr1*-siRNA. (C, n = 3; D-E, n = 6). Data are expressed as mean ± SEM. $^*P$ < 0.05, $^{**}P$ < 0.01, $^{***}P$ < 0.001, vs. PBS-treated MH-S group, $^{###}P$ < 0.001, vs. *Sucnr1*-siRNA transfected MH-S cell line combined with succinate-treated group. **(F)** In MH-S cells, the expression of M1-relate genes was suppressed upon stimulation with 2MeOE2 (100 μmol/L) and LY294002 (10 μmol/L) pretreatment (n = 6). **(G-H)** HIF-1α protein (G) (n = 3) or mRNA (H) (n = 6) expression was downregulated upon LY294002 (10 μmol/L) pretreatment. **(I)** The number of apoptotic MLE-12 cells was reduced upon stimulation with 2MeOE2 (100 μmol/L) and LY294002 (10 μmol/L) pretreatment (n = 3). Data are expressed as mean ± SEM. $^{**}P$ < 0.01, $^{***}P$ < 0.001, versus PBS group; $^{###}P$ < 0.001, vs.succinate-treated group.

Figure 8: Gut microbiota-derived succinate acts as a key mediator of the gut-lung axis in the pathogenesis of intestinal I/R-induced ALI. Schematic diagram illustrating

dysbiosis of microflora related to succinate metabolism (increase in succinate producers and decrease in succinate consumers) and tight junction disruption leading to blood transmission and succinate accumulation in the lung, where succinate exacerbates intestinal I/R-induced ALI by promoting polarization of AMs towards the M1 phenotype, partly through of *Sucnr1*-activated PI3K/AKT/HIF-1α signaling.
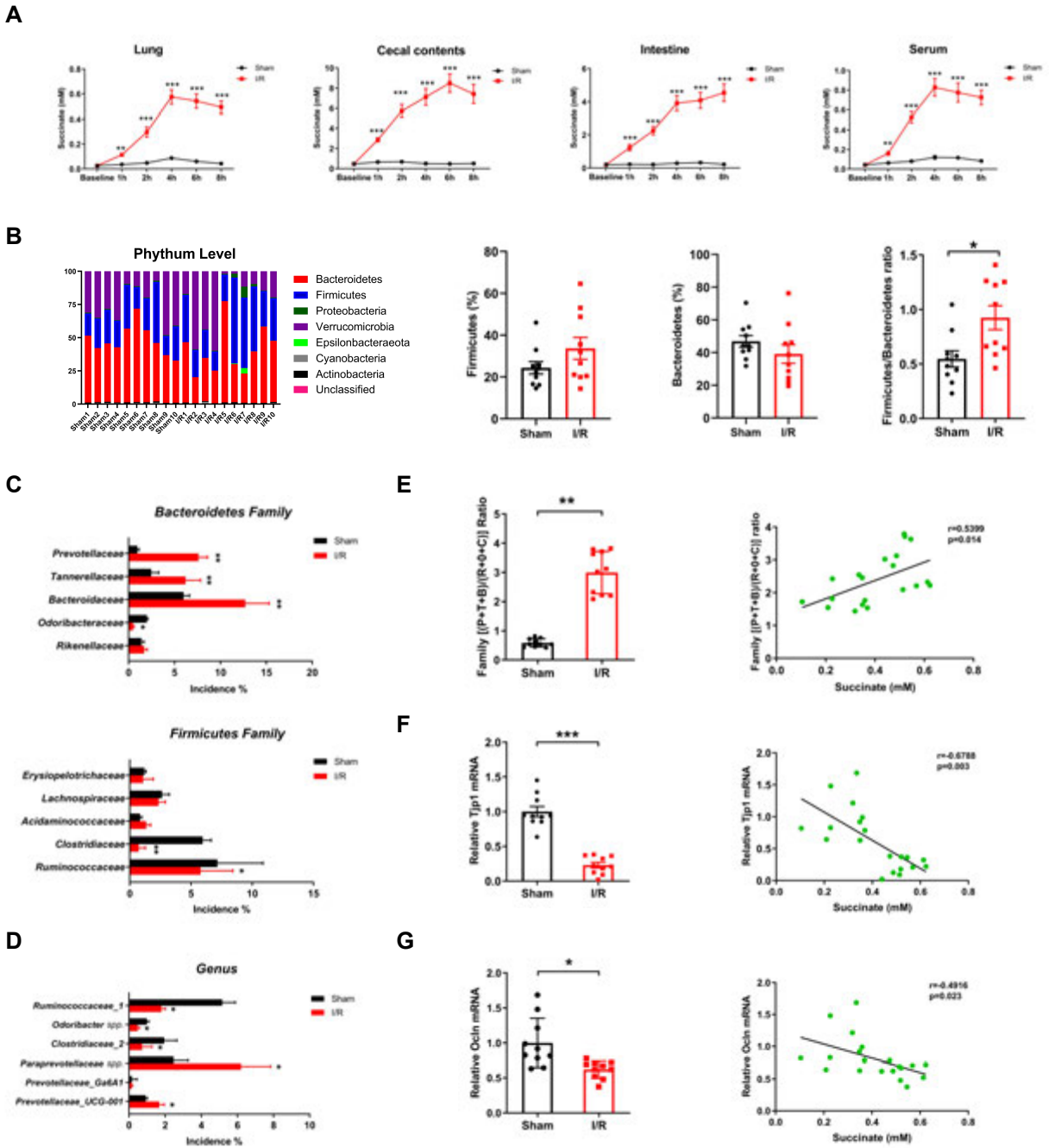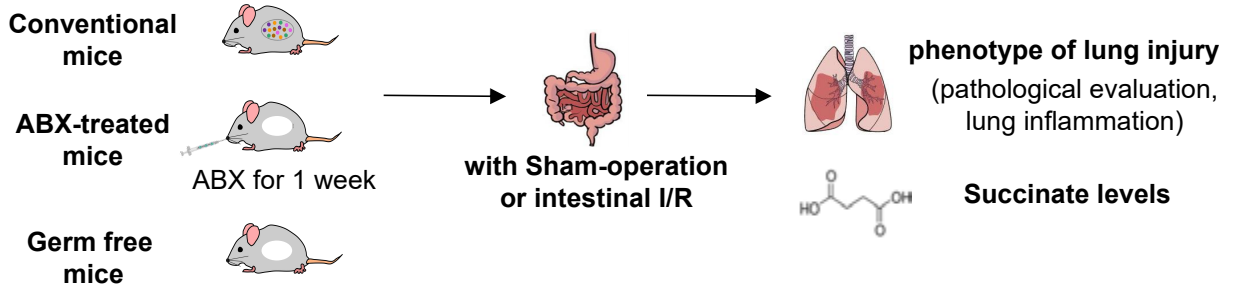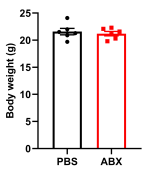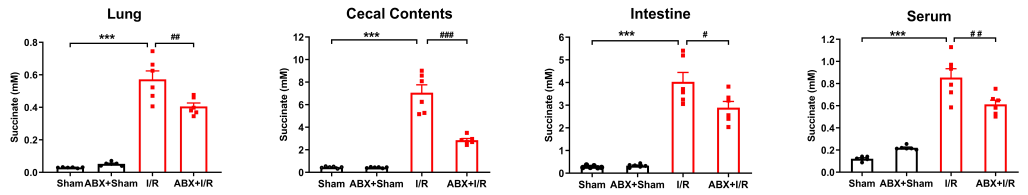
A

B

C

D

E

F

G

Figure 1

Figure 2

A

Ctrl
conventional mice

I/R

Fecal collection at 4 hours of reperfusion

Fecal microbiota transplantation

3 d

Germ-free mice

24-48h

phenotype of lung injury (pathological evaluation, lung inflammation)

HO—C—CH₂—CH₂—C—OH

Succinate levels

B

Ctrl   I/R

24h

48h

C

TNF-α   IL-6   IL-1β

Serum

TNF-α   IL-6   IL-1β

Lung

D

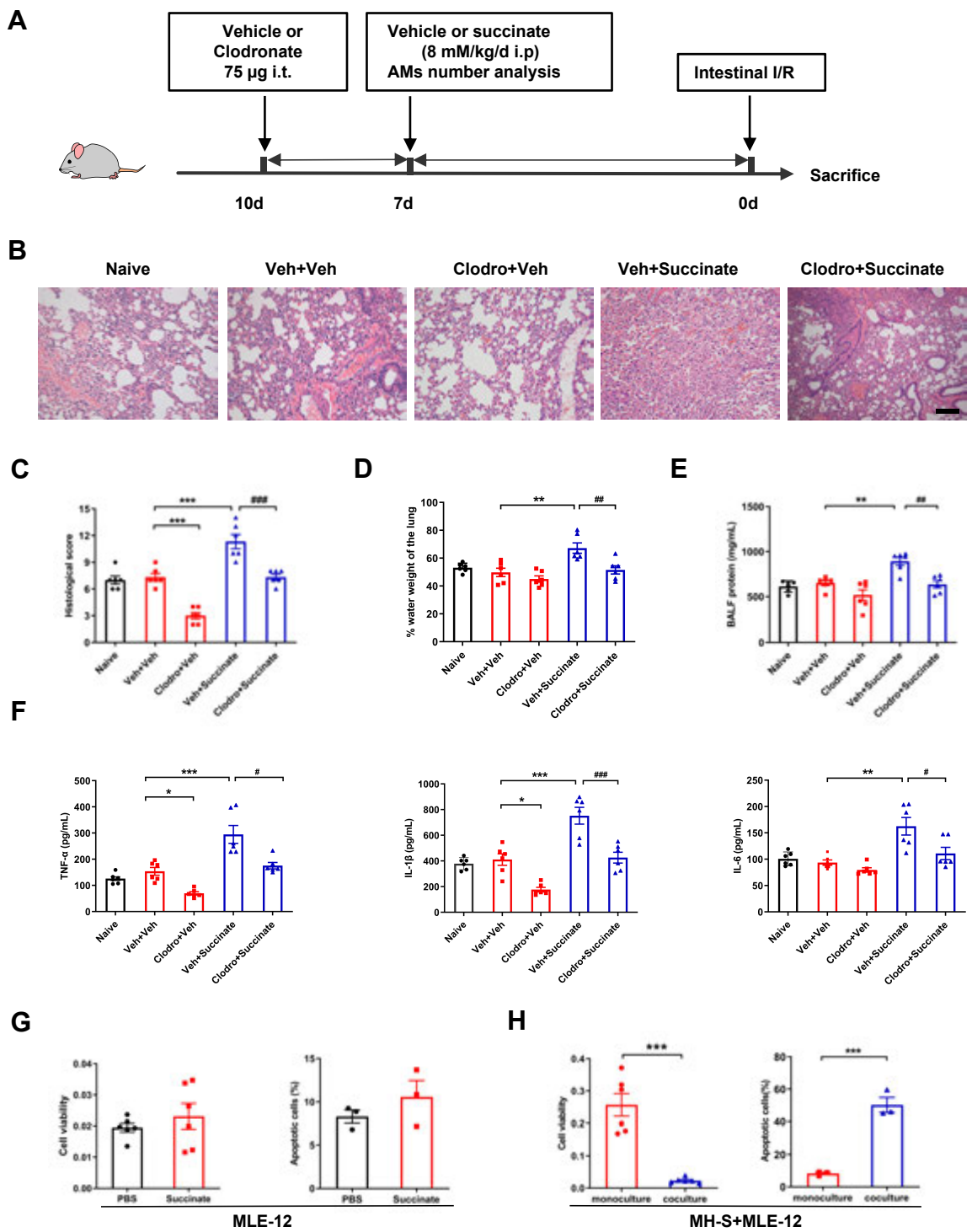Lung   Cecal contents   Intestine   Serum
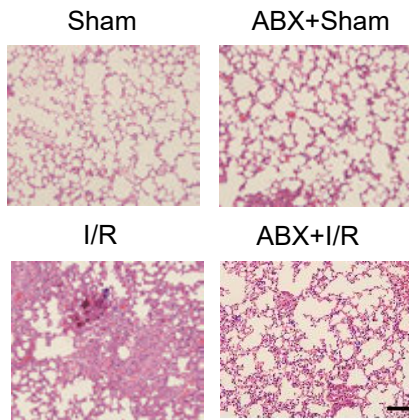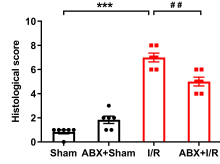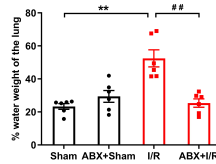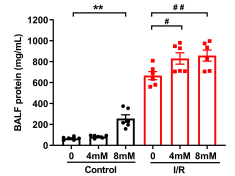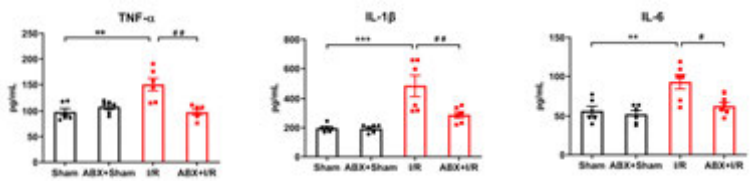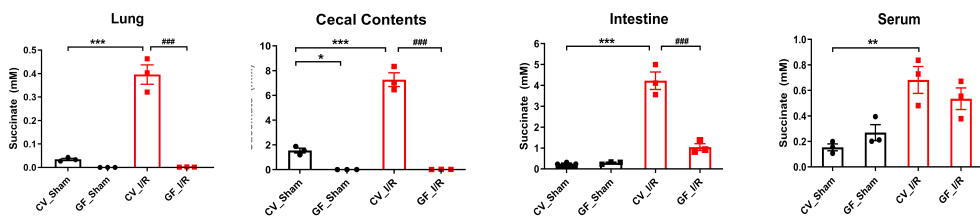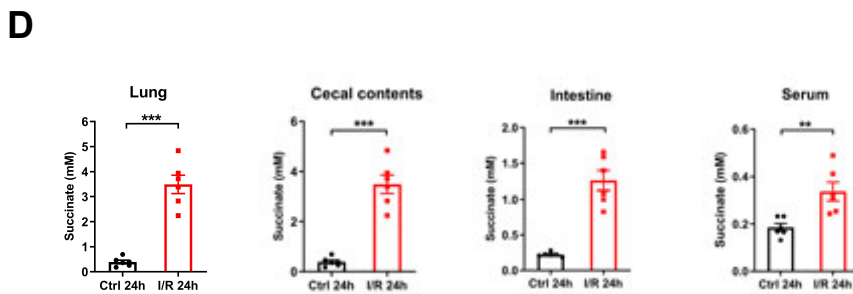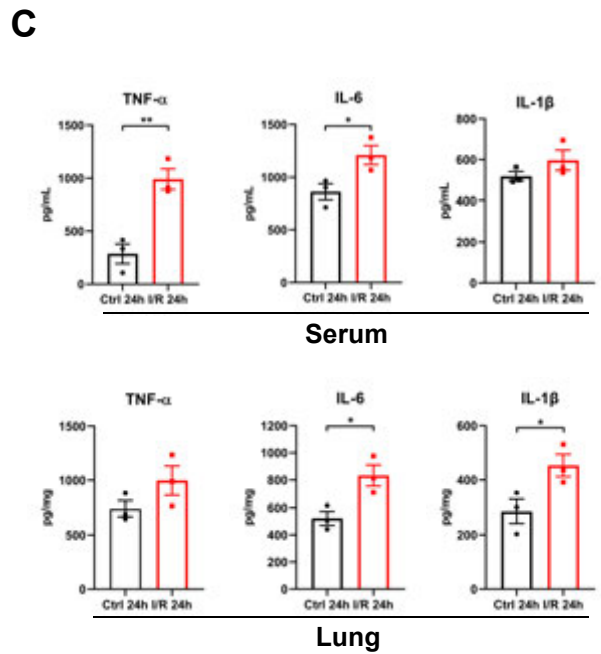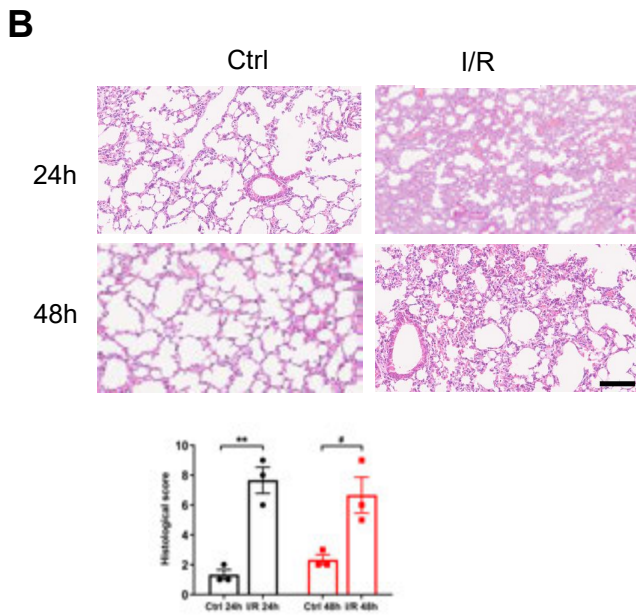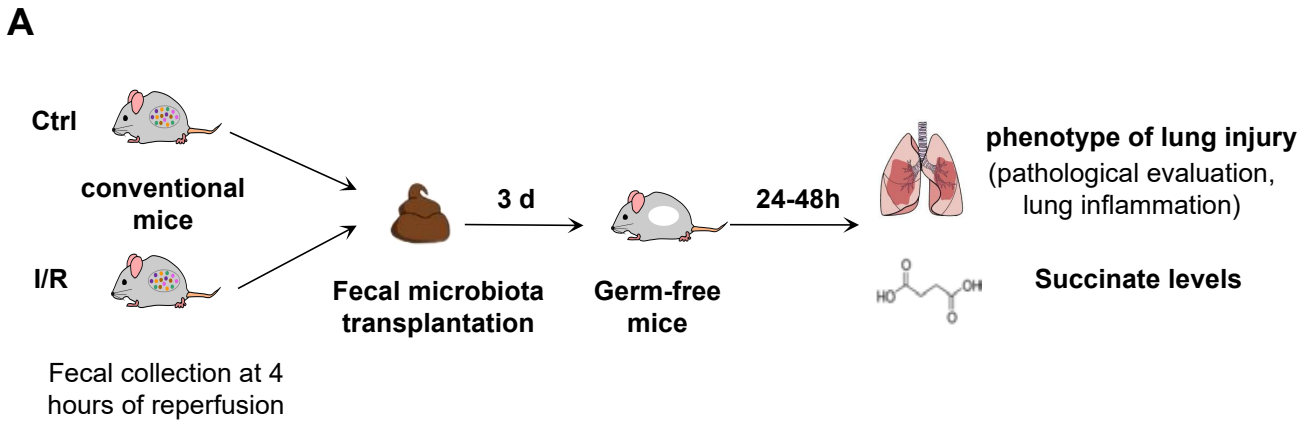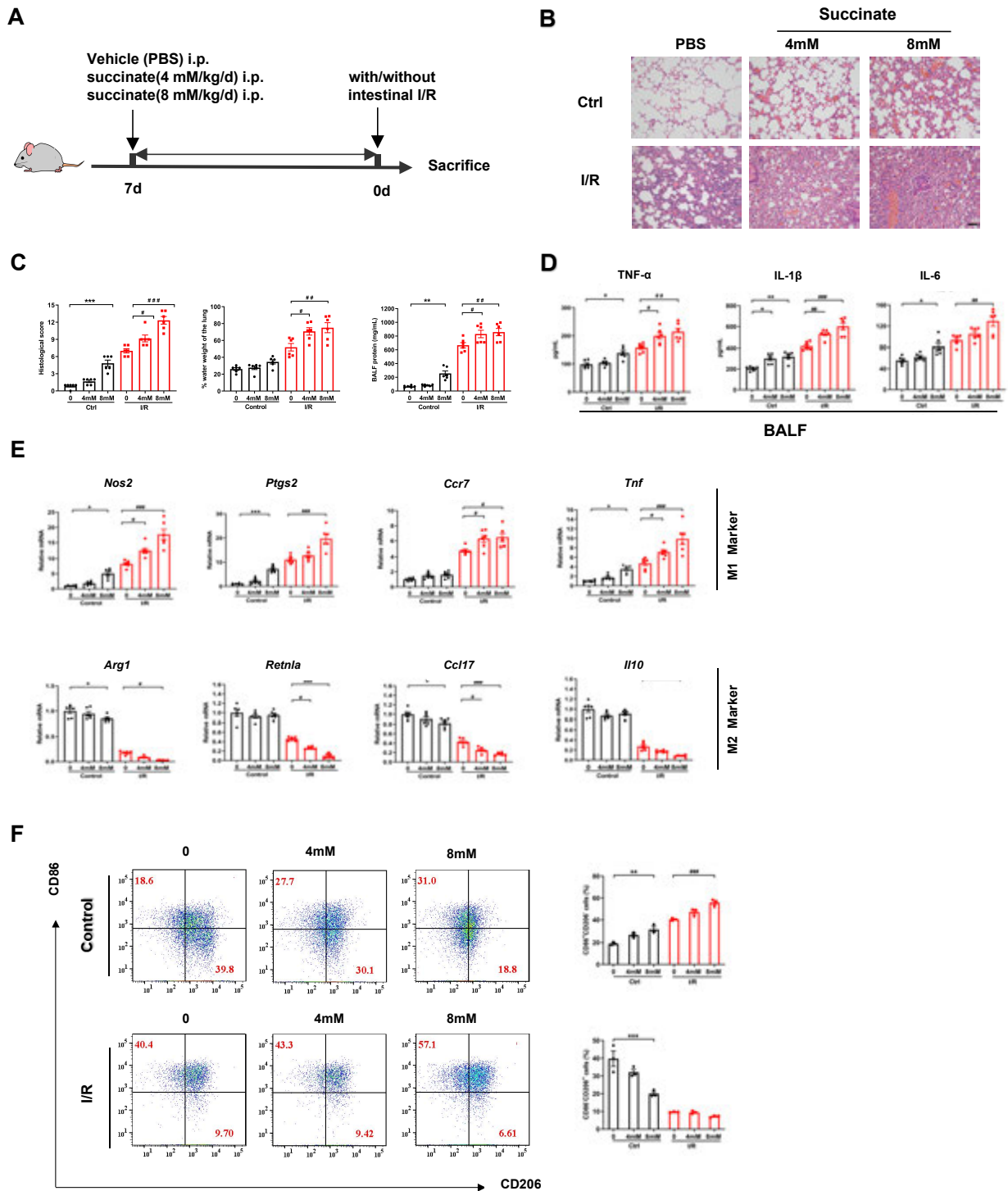
Figure 3

Figure 4

Figure 5

Figure 6

Figure 7

Apoptosis of Alveolar Epithelial Cell

Inflammatory M1-like Alveolar Macrophage

iNOS, Ptgs2
Ccr7, TNF-α

Pro-inflammatory
Cytokines
(TNF-α, *etc.*)

HIF-1α

PI3K/AKT

Intraalveolar
Space

SUCNR1

Succinate

Acute Lung Injury

Gut Microbiota-derived Succinate

Intestinal I/R

Consumers

Succinate

Producers

Microbiota Dybiosis

Tight Junction Disruption
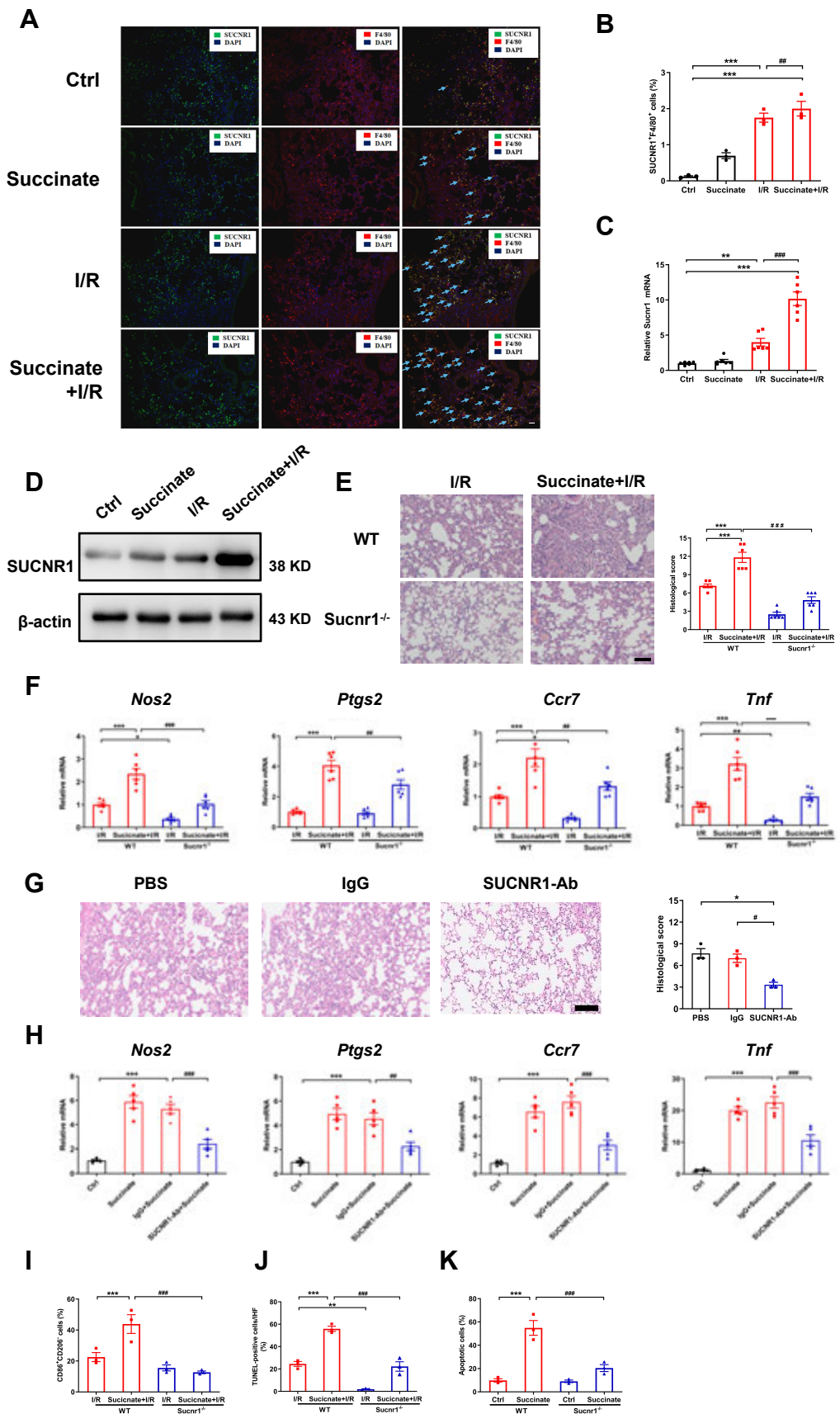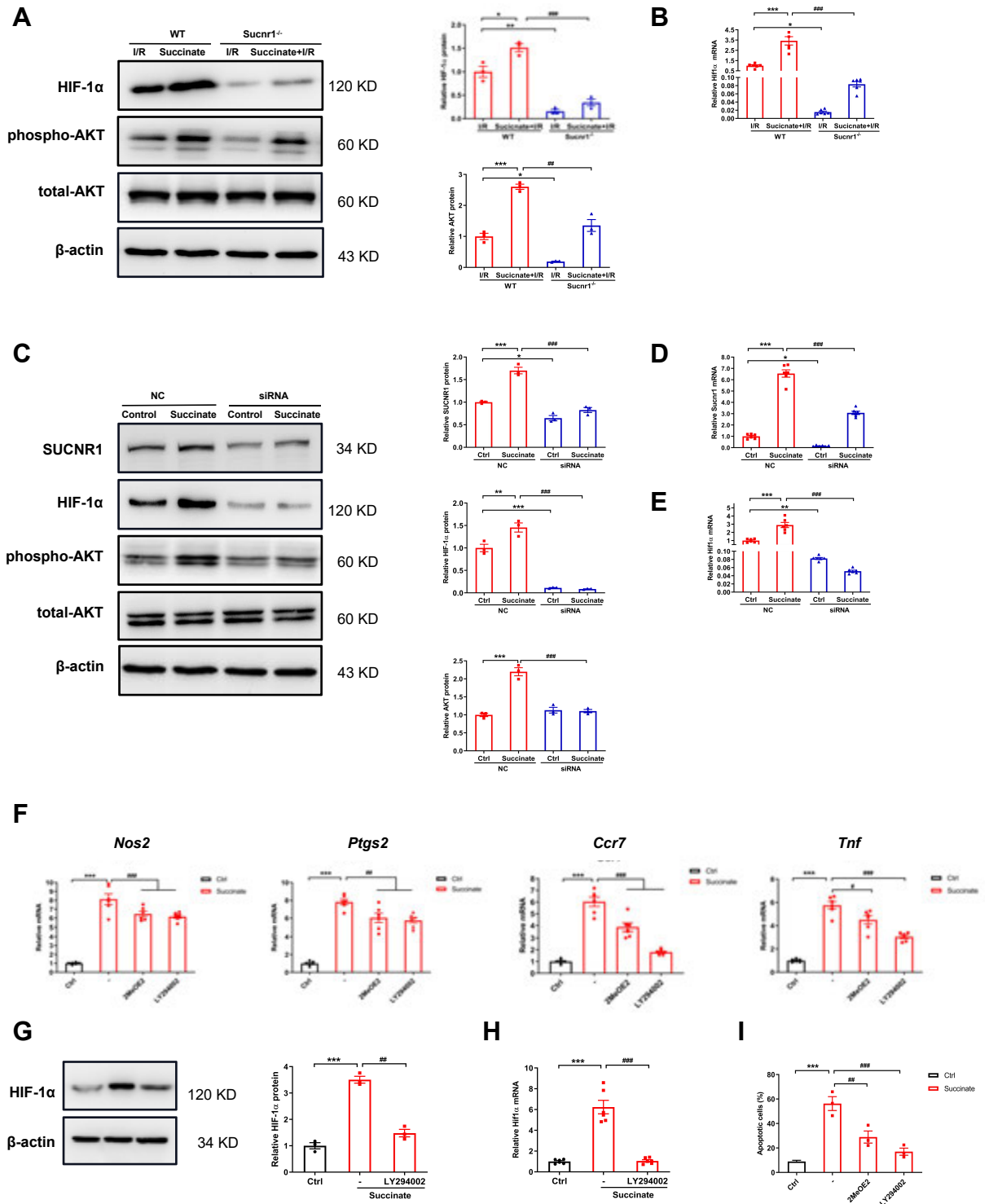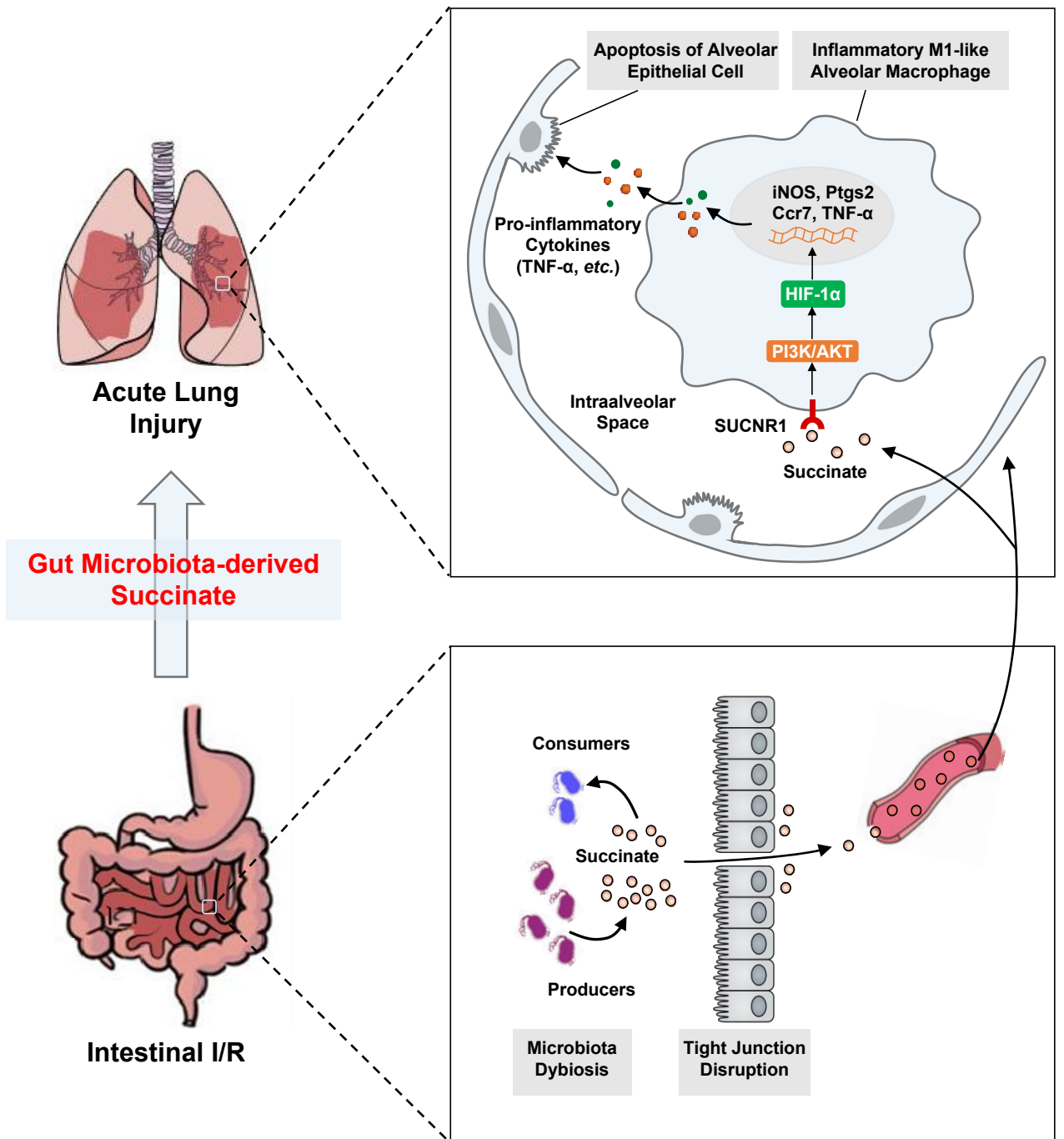
Figure 8

Online Data Supplement

Gut microbiota-derived succinate aggravates acute lung injury after intestinal ischemia/reperfusion in mice

Yi-Heng Wang[1, 2#], Zheng-Zheng Yan[1#], Si-Dan Luo[1], Jing-Juan Hu[1], Mei Wu[1], Jin Zhao[1], Wei-Feng Liu[1], Cai Li[1*], Ke‑Xuan Liu[1*]

[1]Department of Anesthesiology, Nanfang Hospital, Southern Medical University, Guangzhou 510515, Guangdong Province, China.

[2]Department of Anesthesiology, The First Affiliated Hospital, Hengyang Medical School, University of South China, Hengyang 421001, Hunan Province, China.

Supplemental materials and methods

Human subjects

Thirty adult patients who were scheduled for cardiac surgery with cardiopulmonary bypass (CPB) were enrolled in the study between July 2019 and June 2020. Written informed consent were obtained from all participants. Venous blood samples were collected from all patients at various time points: before the operation or induction and 1, 6, 12 and 24 h after the surgery. Plasma succinate levels were determined. The study protocol was approved by the Ethics Committee on Human Studies at Nanfang Hospital, Southern Medical University (Guangdong, China).

Animals

Wild-type (WT) mice were obtained from Beijing HFK Bioscience Co., Ltd. (Beijing, China). *Sucnr1*$^{-/-}$ mice and germ-free (GF) mice were purchased from Cyagen Biosciences Inc (Suzhou, China). All of the male mice, aged 6 – 8 weeks, were maintained on the C57BL/6J genetic background. All mice recieve the same food with standard rodent chows and were free access to drinking water throughout the study. All mice were bred under specific pathogen-free conditions at the Animal Care and Use Committee of Southern Medical University (Guangdong, China). All experimental procedures were carried out in accordance with the National Institutes of Health Guide for the Care and Use of Laboratory Animals. The study protocol was approved by the Animal Ethics Committee at Nanfang Hospital, Southern Medical University (Guangdong, China).

Animal model

A previously described rodent model of intestinal I/R was used in this present study [1]. Briefly, after anesthesia with 4% isofurane, midline laparotomy was performed to exteriorize the small intestine. Ischemia was achieved by occluding the superior mesenteric artery (SMA) with a microvascular clip. After 60 min, the clip was removed to allow reperfusion of the SMA. The cecal contents, distal small intestine, serum and lung tissue were collected at 1, 2, 4, 6, and 8 h after reperfusion. Animals in the sham group underwent the same operation without SMA occlusion. The samples were collected at the same time points as in the I/R group.

Single-housing and co-housing experiments

WT mice were housed under single-housing and co-housing conditions as required. Briefly, 40 mice were randomly assigned into cohorts of single-housing (one per cage, n = 20) or co-housing (in a single cage, n = 20) conditions. Intestinal I/R opeartion and sham operation were performed at 7th day of co-housing or single-housing (n = 10 per group). The samples was collected for subsequent microbial analysis and biochemical measurement at the baseline and different reperfusion time.

Depletion of AMs

For depletion of endogenous AMs, 75 μL clodronate-containing liposome suspension (Yeasen, Shanghai, China) was administered by intratracheal injection 72 h before succinate pre-treatment, based on a previous report [2] and our pilot experiments. Mice of the control group received the same volume of control liposomes. Depletion of AMs was assessed at 72 h after fluorescence staining of BALF cells.

***In Vivo* Neutralization of SUCNR1**

Mice were injected with a singe dose of 100 μL anti-SUCNR1 antibody (Novus Biological; 2.5 μg/g) through the tail vein immediately after one hour of intestinal SMA occlusion [3]. An control IgG isotype (R&D system) and PBS with the same volume were used as control. All antibodies and solutions were sterile, azide-free and low-endotoxin, suitable for in vivo administration.

Bronchoalveolar lavage

Mice were tracheostomized under anesthesia. Briefly, the trachea was exposed by removing the skin of the upper body and neck of mice. The trachea was carefully dissected clean of surrounding connective tissue, and a thread was introduced behind the trachea. An opening of the trachea was made by cutting a small hole on the anterior wall, and a severed 22-gauge needle was inserted through the hole. The thread previously placed behind the trachea was tied around the needle to keep it in place. Bronchoalveolar lavage was performed by gradually instilling 1 mL PBS into the lungs. The PBS was then injected and withdrawn 10 times to ensure thorough sampling of the bronchoalveolar compartment and maximized AM retrieval.

Lung edema assessment

The degree of lung edema was assessed by measurement of lung water contents. After sacrifice with anesthesia, the lungs were removed. The wet weight of the lung was obtained and then the lungs were dried for 72 h at 50℃ and weighed again (dry weight). Dividing the (wet weight-dry weight) by the wet weight gives the lung water contents.

Histological evaluation

H&E staining was performed in formalin-fixated (10% formalin, Biosharp) paraffin-embedded tissue sections sliced at 5 μm thickness. The pathological score was assessed as described previously [4-6]. The stained sections were graded by experienced pathologies in a blinded fashion with regard to the following parameters:

alveolar congestion, hemorrhage, aggregation of neutrophils or leukocyte infiltration, and thickness of the alveolar wall. Each feature was scored on a scale of 0 to 4, where: 0 means no injury, 1 means 25% injured, 2 means 50% injured, 3 means 75% injured and 4 means 100% injured. By adding the scores derived from these four parameters, a composite lung injury score was obtained for each mouse, where 0 meant no lung injury and 16 meant maximal lung injury.

Immunofluorescence

For immunofluorescence staining, lung tissue specimens were deparaffinized for multiplexed staining using the Opal protocol followed by antigen retrieval according to the manufacturer's protocol (Perkin Elmer, Waltham, MA, USA). Following cooling and washing with TBST, nonspecific binding was blocked by incubating the tissue sections with 10% normal goat serum (Boster, Biotech Co., Ltd. Wuhan, China) for 30 min. Tissue sections were then incubated for 1 h at room temperature with the relevant primary antibody, followed by secondary antibody goat anti-rabbit IgG H&L (horseradish peroxidase [HRP] conjugated) (Abcam; 1:4,000). The following primary antibodies and concentrations were used: F4/80 (Cell Signaling Technology; 1:1,000) and SUCNR1 (Novus Biological; 1:500). The tyramide signal amplification (TSA)-dye (Opal 7-Color Manual IHC Kit, Perkin Elmer, Waltham, MA, USA) was applied on tissue sections after washing. Sections were then washed twice with PBS, and nuclei were visualized by mounting the sections in medium containing DAPI. All images were examined under a BX63 Microscope System (Olympus Europa SE & Co. KG) and analyzed by ImageJ software (v 1.52a, NIH, Bethesda, MD, USA).

FAM-succinate fluorescence labeling

Carboxylic acid fluorescein (FAM) were used to modify succinate to construct a fluorescence-labeling molecular, FAM-succinate, which was synthesized by Genebio Biotech (Guangzhou, China). Once the post-synthesis modification completed, the molecular structure and representative mass spectra was confirmed (Figure S2A-B). Mice were then treated with FAM-succinate (150 mM, 100 μL) intragastrically one day before sham-operation or I/R-operation. Subsquently, blood, ileum and lung samples were harvested for visualizing in vivo fluorescence intensity.

TUNEL assay

Apoptotic cells were visualized using a red fluorescent-tagged TUNEL kit (Roche, Penzberg, Germany) following dewaxing and incubation with proteinase K. Cell nuclei were labeled with blue DAPI. Tetramethylrhodamine-labeled nucleotides indicating DNA strand breaks in apoptotic cells were visualized as red staining against a blue background under a florescent microscope.

Isolation of primary AMs

Primary murine AMs were isolated from BALF obtained by lavage with 37℃ PBS containing 100 mM ethylenediaminetetraacetic acid (EDTA), and the purification was performed using density centrifugation [7]. Briefly, BALF samples were centrifuged, washed with Hanks balanced salt solution (HBSS), layered over a Percoll gradient (75%,

25%), and centrifuged at 1060 g for 30 min. Samples of the 25%–75% interface were revealed to contain more than 90% macrophages.

Cell culture

MH-S cells (a murine AM cell line) and MLE-12 cells (an alveolar epithelial cell line) were obtained from American Type Culture Collection (ATCC) and cultured in complete RPMI-1640 medium containing 10% fetal bovine serum (FBS), L-glutamine, penicillin, and streptomycin at 37℃ in humidified air containing 5% CO_2.

Transient cell transfection with *Sucnr1*

MH-S cells were transfected with siRNAs (50 nM) targeting mouse *Sucnr1* and negative control (NC) siRNAs (Sangon Biotech, Shanghai, China) the using Lipofectamine™ 3000 Transfection Reagent (Invitrogen, Waltham, MA, USA) according to the manufacturer's instructions. The siRNA sequences are listed in Table S3. The mRNA and protein expression levels of SUCNR1 were analyzed to determine the efficiency of transfection.

Co-culture assay and apoptosis analysis

MH-S cells or primary AMs isolated from the lung in *Sucnr1*^{-/-} mice were cultured on a 0.4-μm Transwell membrane insert (EMD Millipore, Danvers, MA), and MLE-12 cells were cultured in wells of a 12-well culture plate. After 24-h in co-culture, the MLE-12 cells were collected for assessment of apoptosis using the Annexin-V-FITC Apoptosis Detection Kit (Vazyme Biotech Co., Ltd. Nanjing, China). The assay was performed according to the manufacturer's instructions. Annexin-V–positive cells were considered

apoptotic, and the analysis was performed using FlowJo software (v10.0, Tree Star, Ashland, OR, USA).

Cell viability assay

Confluent MLE-12 cells ($5×10^3$/plate) loaded in 96-well plates were maintained in Dulbecco's Modified Eagle's Medium (DMEM) with 10% FBS, and then treated with PBS or succinate (1 mM) or co-cultured with succinate-induced polarized AMs. After 24 h, cells were treated with MTT reagent (10 µl) for 4 h at 37℃ and then with solubilization solution (100 µl) at 37℃ overnight. A Bio-Rad microplate reader (Model-680, Hercules, CA, USA) was used to measure the absorbance of the solution in each well at 490 nm. Wells containing only culture medium but no cells served as controls. All experiments were repeated five times to ensure consistent results.

Flow cytometry

BALF samples were fixed in 4% formaldehyde immediately after lavage. Cells were then suspended in FBS (BD Biosciences, USA) at a concentration of 10^6 cells per 100 µl. FcγR was blocked, and cells were stained with either specific antibodies against surface antigens in PBS with 2% FBS or intracellular antigens with the Intracellular Fixation & Permeabilization Buffer Set (BD Biosciences, USA) according to recommended protocols. A Fortessa XII cytometer (BD Biosciences, USA) was used for flow cytometry. Data were collected and analyzed with Flow Jo v10 software.

Enzyme-linked immunosorbent assay (ELISA)

The levels of TNF-α, IL-1β and IL-6 in BALF were measured using commercially available ELISA kits (Boster Biotech, Wuhan, China) according to the manufacturer's protocols.

RT-PCR analysis

Extraction of total RNA from AMs or tissues was carried out using the TRIzol reagent (Invitrogen). Reverse transcription of RNA into cDNA was performed using a PrimeScript RT Kit (Toyobo). qPCR was performed on a BioRad iQ5 real-time PCR machine using SYBR Green PCR Master Mix (Toyobo). GAPDH was used as the housekeeping gene control. The primers used to amplify the major targeted genes are listed in Table S3.

Western blotting

Cell lysates from primary AMs or MH-S cells were centrifuged at 15,000g for 20 min at 4℃ to eliminate cell debris. After protein extraction, the total protein concentration was determined using the Bradford Protein Assay (Keygen Biotech, Nanjing, China) according to the manufacturer's instructions. Total protein (50 μg per sample) was separated on gels and then electroblotted onto polyvinylidene difluoride (PVDF) membranes. The membranes were probed overnight with the relevant primary antibodies: anti-SUCNR1 (1:500), anti-HIF-1α (1:1,000), anti-phospho-AKT (1:2,000), anti-total-AKT (1:1,000), and anti-β-actin (1:500). This was followed by incubation with secondary HRP-conjugated mouse antibodies (1:10,000). Membranes were developed using an enhanced chemiluminescence system (Thermo Fisher Scientific). Bands were analyzed and quantified using the ImageJ software (version 1.52a).

Supplemental references:

1．Zhang XY, Liang HS, Hu JJ, Wan YT, Zhao J, Liang GT, Luo YH, Liang HX, Guo XQ, Li C, Liu WF, Liu KX. Ribonuclease attenuates acute intestinal injury induced by intestinal ischemia reperfusion in mice. *International immunopharmacology* 2020: 83: 106430.

2．Wang L, Zhang H, Sun L, Gao W, Xiong Y, Ma A, Liu X, Shen L, Li Q, Yang H. Manipulation of macrophage polarization by peptide-coated gold nanoparticles and its protective effects on acute lung injury. *Journal of nanobiotechnology* 2020: 18(1): 38.

3．Liberale L, Bonetti NR, Puspitasari YM, Schwarz L, Akhmedov A, Montecucco F, Ruschitzka F, Beer JH, Lüscher TF, Simard J, Libby P, Camici GG. Postischemic Administration of IL-1α Neutralizing Antibody Reduces Brain Damage and Neurological Deficit in Experimental Stroke. *Circulation* 2020: 142(2):187-189.

4．Gong S, Yan Z, Liu Z, Niu M, Fang H, Li N, Huang C, Li L, Chen G, Luo H, Chen X, Zhou H, Hu J, Yang W, Huang Q, Schnabl B, Chang P, Billiar TR, Jiang Y, Chen P. Intestinal Microbiota Mediates the Susceptibility to Polymicrobial Sepsis-Induced Liver Injury by Granisetron Generation in Mice. *Hepatology* (Baltimore, Md) 2019: 69(4): 1751-1767.

5．Cox R Jr, Phillips O, Fukumoto J, et al. Enhanced Resolution of Hyperoxic Acute Lung Injury as a result of Aspirin Triggered Resolvin D1 Treatment. Am J Respir Cell Mol Biol 2015:53(3):422-435.

6．Robertson JA, Sauer D, Gold JA, Nonas SA. The role of cyclooxygenase-2 in

mechanical ventilation-induced lung injury. Am J Respir Cell Mol Biol 2012:47(3):387-394.

7. Janssen WJ, McPhillips KA, Dickinson MG, Linderman DJ, Morimoto K, Xiao YQ, Oldham KM, Vandivier RW, Henson PM, Gardai SJ. Surfactant proteins A and D suppress alveolar macrophage phagocytosis via interaction with SIRP alpha. *Am J Respir Crit Care Med* 2008: 178(2): 158-167.

Table S1: Demographic and clinical characteristics of the study population (n=30)

Characteristics	
Sex (male/female)	14/16
Age (years)	55.5±1.9
BMI (kg/m^2)	23.7±1.3
ASA physical status, II, III	3/27
Perioperative EF (%)	58.7±1.6
Duration of anesthesia (min)	315.8±8.4
Operation time (min)	263.7±7.8
CPB time (min)	132.4±7.2
Mechanical ventilation time (h)	24.5±2.3
ICU stay (h)	90.3±10.5
Blood loss (ml)	345.0±15.6
Blood transfusion (ml)	434.7±42.1
In-hospital stay (days)	20.8±1.4

Data are presented as the mean ± SEM or in parameter counts.

ASA, American Society of Anesthesiologists; BMI, body mass index;

CPB, cardiopulmonary bypass; EF, ejection fraction.

Table S2: Antibodies and Reagents

REAGENT or RESOURCE	SOURCE	IDENTIFIER
Antibodies		
Anti-SUCNR1	Novus	NBP1-00861
Rat anti-mouse F4/80	Abcam	ab53444
Anti-HIF1α	Cell Signaling	36169
Anti-phospho-Akt(Ser473)	Cell Signaling	4060
Anti-Akt	Cell Signaling	4691
Anti-phospho-p38 MAPK (Thr180/Tyr182)	Cell Signaling	4511
Anti-p38 MAPK	Cell Signaling	8690
Anti-phospho-NF-κB p65 (Ser536)	Cell Signaling	3033
Anti-NF-κB p65 (Ser536)	Cell Signaling	8242S
HRP-goat anti-rabbit IgG(H+L）	Proteintech	SA00001-2
Rabbit IgG control	R&D systems	AB-105-C
FITC anti-mouse F4/80 (Clone BM8)	eBioscience	11-4801-82
PE anti-mouse CD11c (Clone N418)	eBioscience	12-0114-81
PE cyanine7 anti-mouse CD86 (Clone GL1)	eBioscience	25-0862-82
APC anti-mouse CD206 (Clone MR6F3)	eBioscience	17-2061-82
Purified rat anti-mouse CD16/CD32(Mouse BD Fc Block™)	BD Biosciences	553141
Chemicals & Reagents		
Succinic acid BioReagent	Sigma-Aldrich	S9512
Ampicillin	Macklin	69-53-4
Neomycin	Macklin	1405-10-3
Metronidazole	Macklin	443-48-1
Vancomycin	Macklin	1404-90-6
Clodronate liposomes	Vrije Universiteit Amsterdam	40337ES08

Control liposomes (PBS)	Yeasen Biotech	40338ES08
2-MeOE2	Selleck	S1233
Bay11-7082	Sigma-Aldrich	B5556
LY294002	Beyotime	S1737
SB202190	Macklin Biotech	S854645
Percoll gradient	Solarbio Science & Technology	P8370
RPMI 1640	Thermo Fisher	11875085
Trypsin 0.25% EDTA	Thermo Fisher	25200072
Fetal bovine serum	Thermo Fisher	10099141
Stain buffer FBS	BD Biosciences	554656
DAPI	Roche	216276
FAM-succinate	Genebio Biotech	

Key Commercial Assays

Mouse TNF-α ELISA kit	Boster Biotech	EK0527
Mouse IL-6 ELISA kit	Boster Biotech	EK0411
Mouse IL-1β ELISA kit	Boster Biotech	EK0394
Cytofix/Cytoperm Soln kit	BD Biosciences	554714
Annexin-V-FITC apoptosis detection kit	Vazyme Biotech	A211-02
TUNEL apoptosis detection kit	Roche	11684817910
SYBR® Green Realtime PCR Master Mix	Toyobo	QPK-201
Lipofectamine 3000	Thermo Fisher	L3000001

Cell Lines

Mouse cell line: MH-S	ATCC	CRL-2019
Mouse cell line: MLE-12	ATCC	CRL-2110

**Table S3. siRNA sequences and primer sequences used for RT-qPCR**

siRNA sequences used for *Sucnr1* silencing	
Sucnr1 siRNA	5'-GAAUCAACAAGCAGCCAAUUTdTdT-3' (sense)
	5'-AUUGGCUGCUUGUUGCUUCTTdTdT-3'(antisense)
Scramble control	5'-CGAGGAGACUUCCGAAUCUAUdTdT-3'(sense)
	5'-ACGUGACACGUUCGGAGAAUTdTdT-3'(antisense)
Primer sequences used for RT-PCR analysis of *ZONAB*	
Sucnr1	5'-CATATCATGCGCAATTTGAGGA-3'(forward)
	5'-GCCGTGTCAGTGTGTATATAGA-3'(reverse)
Hif1α	5'-GAATGAAGTGCACCCTAACAAG-3'(forward)
	5'-GAGGAATGGGTTCACAAATCAG-3'(reverse)
Nos2	5'-TTCTGTGCTGTCCCAGTGAG-3'(forward)
	5'-TGAAGAAAACCCCTTGTGCT-3'(reverse)
Ptgs2	5'-ATTCCAAACCAGCAGACTCATA-3'(forward)
	5'-CTTGAGTTTGAAGTGGTAACCG-3'(reverse)
Ccr7	5'-GATGACTACATCGGCGAGAATA-3'(forward)
	5'-ACGAAGCAGATGACAGAATACA-3'(reverse)
Tnf	5'-AGGGTCTGGGCCATAGAACT-3'(forward)
	5'-CCACCACGCTCTTCTGTCTAC-3'(reverse)
Arg1	5'-CATATCTGCCAAAGACATCGTG-3'(forward)
	5'-GACATCAAAGCTCAGGTGAATC-3'(reverse)
Retnla	5'-ATCGTGGAGAATAAGGTCAAGG-3'(forward)
	5'-TTGACACTAGTGCAAGAGAGAG-3'(reverse)
Il10	5'-TTCTTTCAAACAAAGGACCAGC-3'(forward)
	5'-GCAACCCAAGTAACCCTTAAAG-3'(reverse)
Ccl17	5'-GATTACTTCAAAGGGGCCATTC-3'(forward)
	5'-GCCTTCTTCACATGTTTGTCTT-3'(reverse)
Tjp1	5'-AGAGACAAGATGTCCGCCAG-3'(forward)
	5'-TGCAATTCCAAATCCAAACC-3'(reverse)
Ocln	5'-CATTTATGATGAACAGCCCC-3'(forward)
	5'-GGACTGTCAACTCTTTCCGC-3'(reverse)
18S	5'-CGATCCGAGGGCCTCACTA-3'(forward)
	5'-AGTCCCTGCCCTTTGTACACA-3'(reverse)

RT-PCR, reverse transcription polymerase chain reaction; siRNA, small interfering RNA.
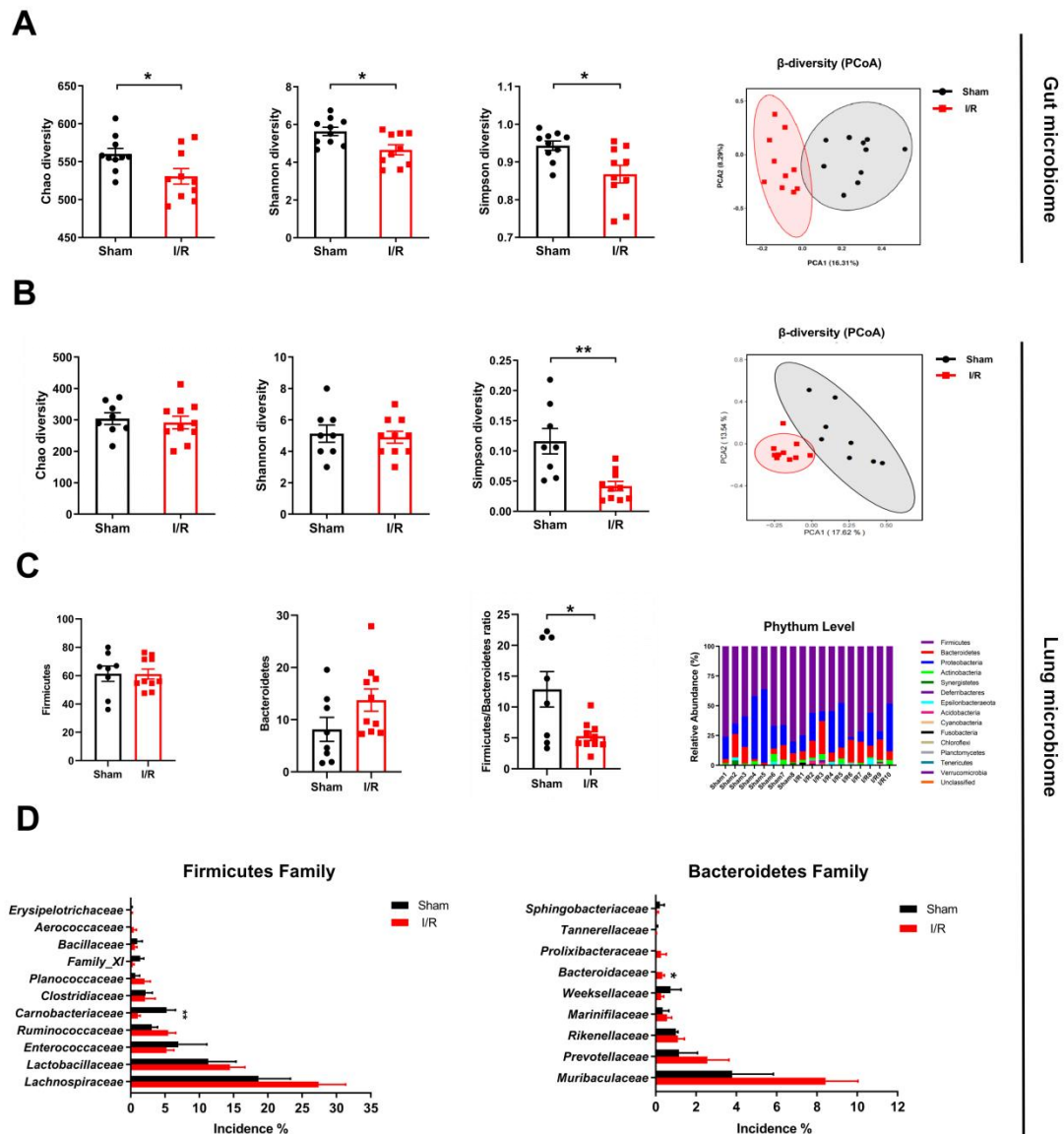
Figure S1: Elevated lung succinate during intestinal I/R was associated with the imbalance of succinate-producing and -consuming bacteria in the gut of co-housed mice. (A-B) The alpha and beta diversity of gut (A) and lung microbiota (B) declined after intestinal I/R. (**C**) Lung microbiota composition at phylum levels during intestinal I/R. (**D**) Representative species of Bacteroidaceaes family and Firmicutes family in lung microbial community. (A) n = 10; (B–D) n = 8-10. Data are expressed as mean ± SEM, $^*P$ < 0.05, $^{**}P$ < 0.01, vs. sham group.
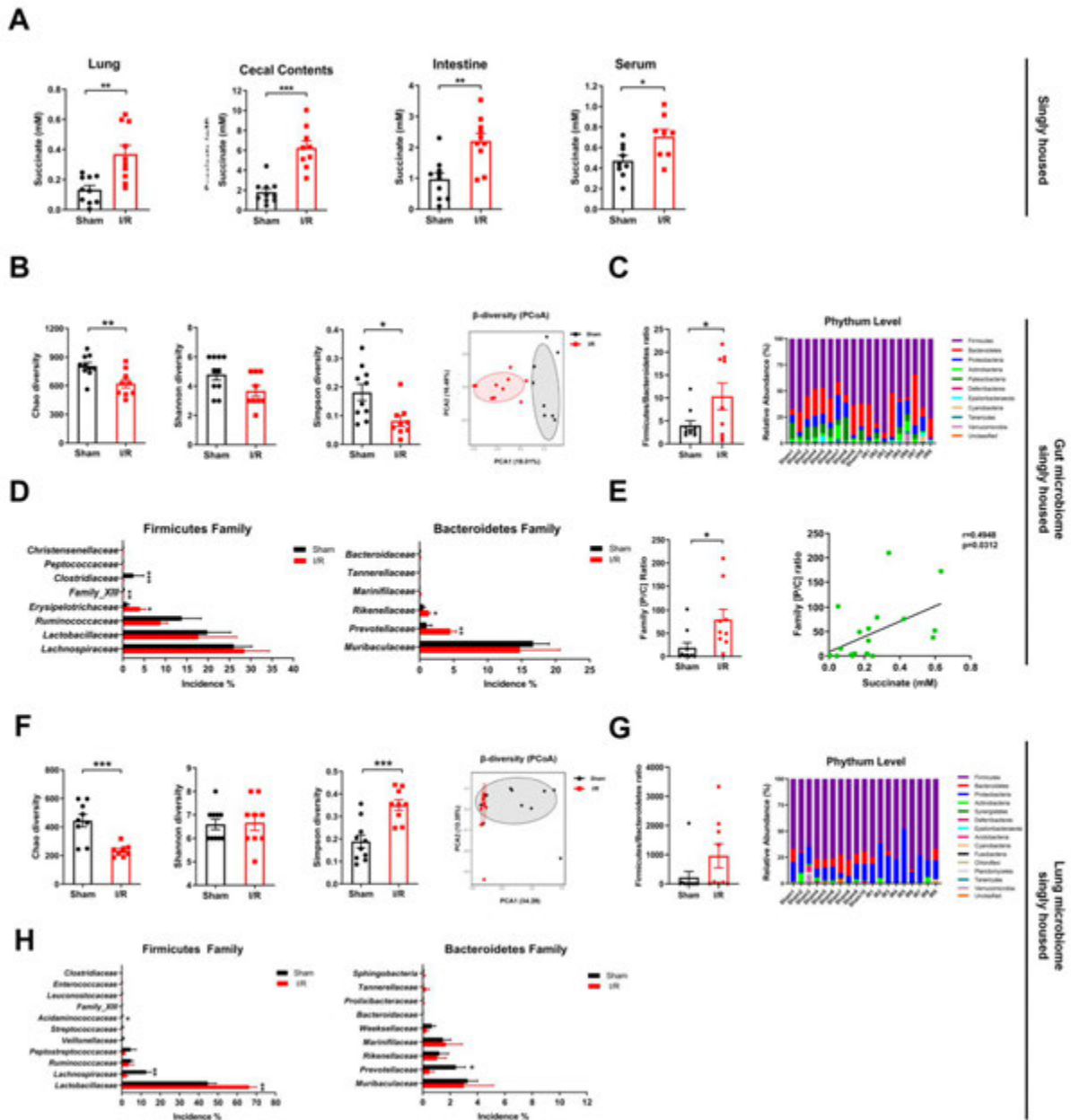
Figure S2: Elevated lung succinate was associated with the imbalance of succinate-producing and -consuming bacteria in the gut of singly housed mice. (**A**) The alterations of succinate levels in the lung, cecal contents, intestine and serum after 1, 2, 4, 6, or 8 h of reperfusion.(*n* = 8-10, sham group vs. I/R group). (**B-C; F-G**) The alpha and beta diversity, and microbial composition at the phylum level in the gut microbiota

(B-C) , and the lung microbiota (F-G) of single-housed mice underwent intestinal I/R. (**D; H**) Representative species of Bacteroidaceaes family and Firmicutes family in gut (F), and lung (H) microbial community.(**E**) The pulmonary succinate level was positively correlated with the ratio between succinate producers (Prevotellaceae) and succinate consumers (Clostridiaceae, C) [(P)/(C) ratio]. (B–H) *n* = 9-10. Data are expressed as mean ± SEM, *P < 0.05, **P < 0.01, ***P < 0.001,vs. sham group.

A

Structure of FAM-succinate
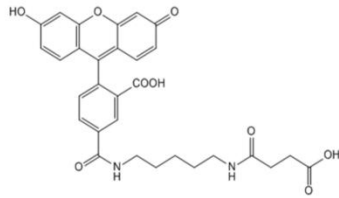
Chemical Formula: $C_{30}H_{28}N_2O_9$
Molecular Weight: 560.55
m/z: 560.18 (100.0%), 561.18 (33.5%), 562.19 (5.3%), 562.18 (2.1%), 563.19 (1.2%)
Elemental Analysis: C, 64.28; H, 5.03; N, 5.00; O, 25.69

B

MS of FAM-succinate
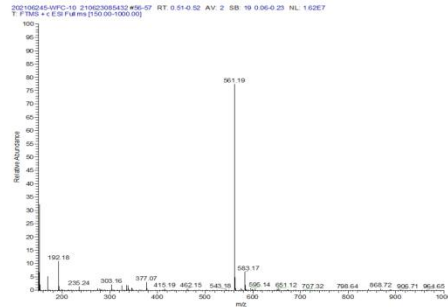
C
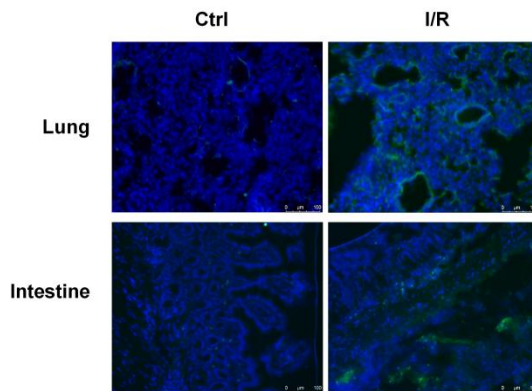
D
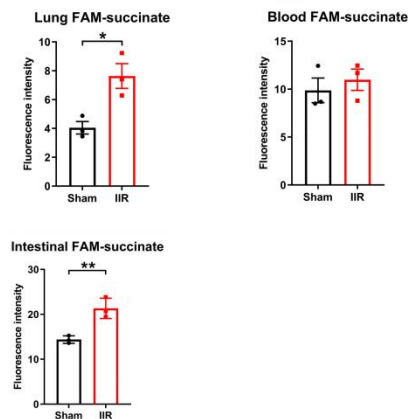
Figure S3: Succinate is probably an important mediator derived from gut microbiota that promotes intestinal I/R-induced ALI through the gut-lung axis. (**A**) The molecular structure of FAM-succinate. (**B**) Representative mass spectra of FAM-succinate. (**C**) Mice treated with FAM-succinate (150 mM) intragastically presented higher levels of fluorescence signal intensity in the gut and lung after intestinal I/R (n = 3). Data are expressed as mean ± SEM, *P < 0.001, **P < 0.01, vs. PBS group.
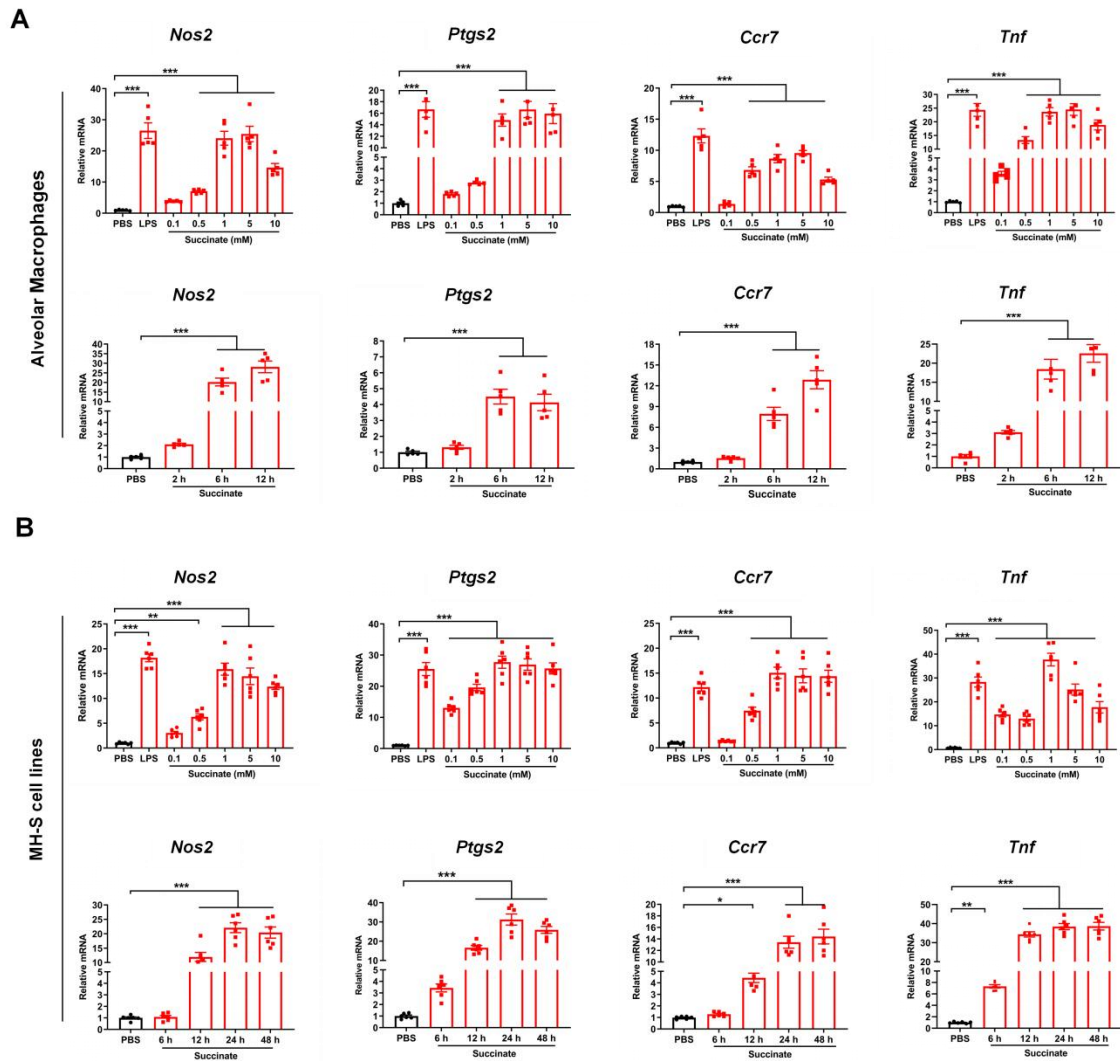
Figure S4: Succinate polarized AMs towards M1 phenotype and aggravated lung injury after intestinal I/R. Succinate polarized AMs towards M1 phenotype. In primary AMs (**A**) and MH-S cells (**B**), succinate increased the mRNA expression of M1 marker genes (*Nos2, Ptgs2, Ccr7,* and *Tnf*) in a dose- and time-dependent manner (*n* = 6). Data are expressed as mean ± SEM, ***P < 0.001, vs. PBS group.
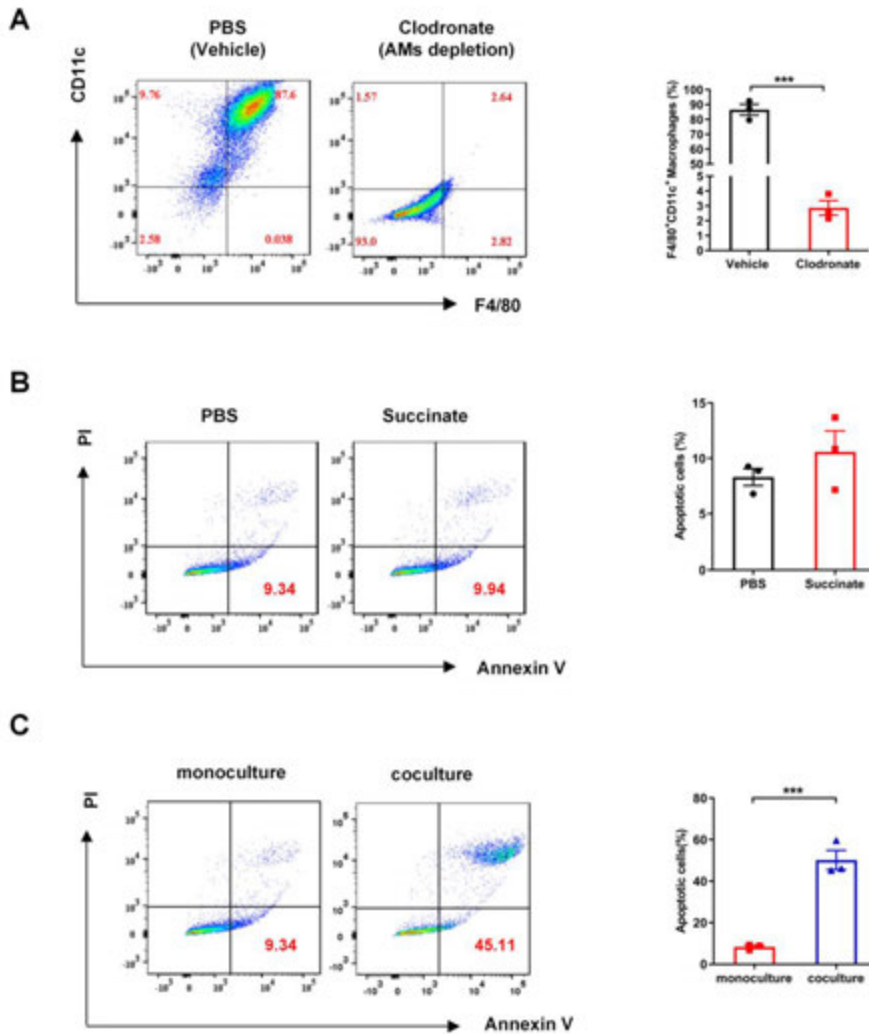
Figure S5: Activation of AMs was essential for succinate-mediated lung injury during intestinal I/R. (A) The number of F4/80^{+}CD11c^{+} macrophages in the lung was significantly reduced after clodronate treatment (*n* = 3). Data are expressed as mean ± SEM, ***P* < 0.001, vs.vehicle group. **(B)** Succinate had no effect on the apoptosis of MLE-12 cells (*n* = 3). Data are expressed as mean ± SEM. ***P* < 0.001, vs. PBS group. **(C)** Co-culture with succinate-induced polarized MH-S cells increased the number of apoptotic MLE-12 cells (*n* = 3). Data are expressed as mean ± SEM. ***P* < 0.001, vs. monoculture group.
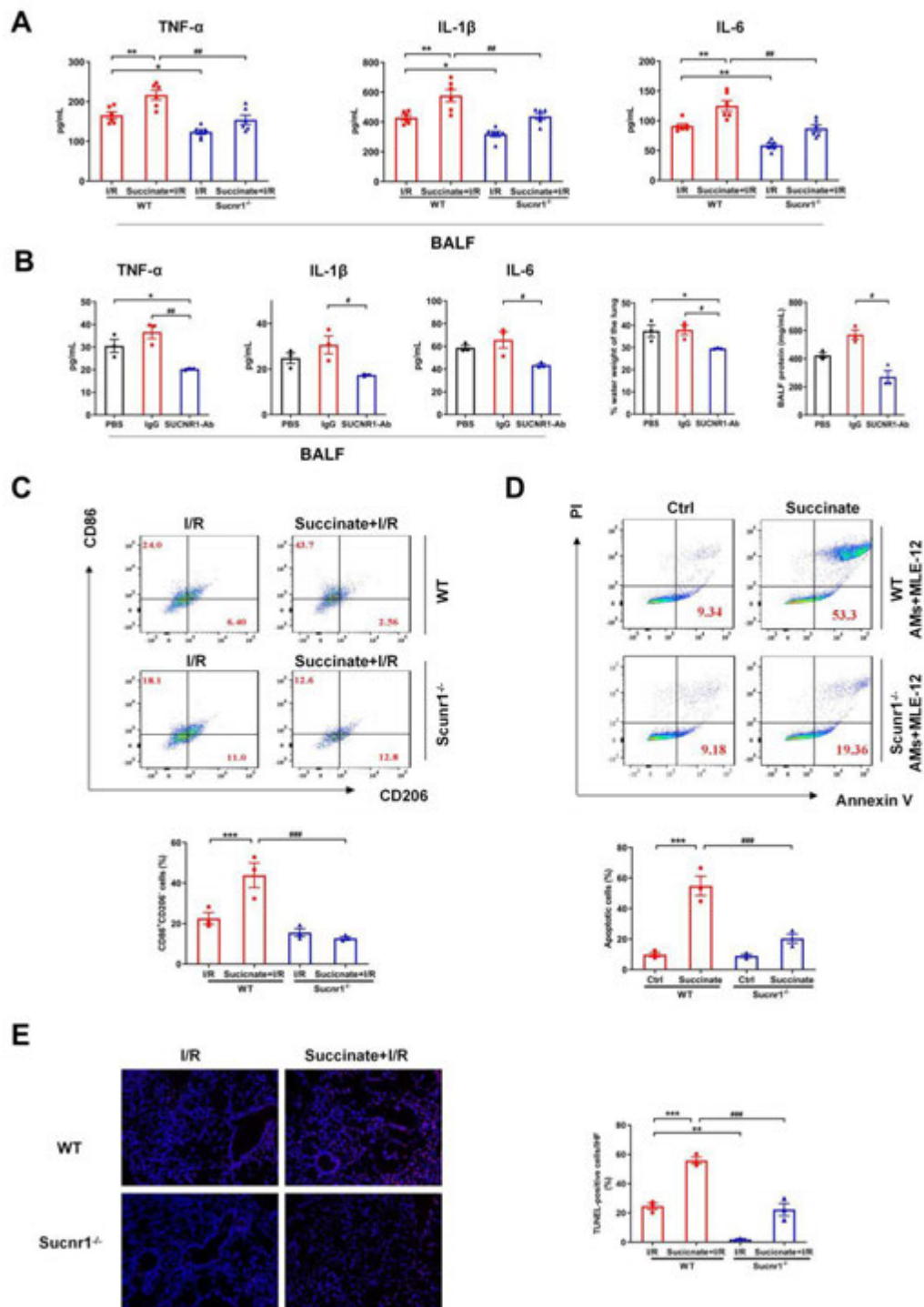
Figure S6: SUCNR1 signaling mediated succinate-induced AM polarization and lung injury after intestinal I/R. (A) *Sucnr1* deficiency attenuated succinate-induced

lung inflammation and the levels of pro-inflammatory cytokines (n = 6). Data are expressed as mean ± SEM. $^{*}P < 0.05,^{**}P < 0.01,$ $^{***}P < 0.001$, vs. WT mice I/R group; $^{##}P < 0.01$, vs. WT mice with succinate+I/R group. **(B)** SUCNR1 antibody reduced lung inflammation, BALF protein levels and the degree of lung edema (*n* = 3). Data are expressed as mean ± SEM. $*P < 0.05$, vs. PBS group; $^{#}P < 0.05$, $^{##}P < 0.01$, vs. IgG group. **(C)** *Sucnr1* deficiency increased the percentage of CD86^{+}CD206^{-} M1 macrophages observed during intestinal I/R (*n* = 3). Data are expressed as mean ± SEM. $^{***}P < 0.001$, vs. WT mice I/R group; $^{###}P < 0.001$, vs. WT mice with succinate+I/R group. **(D)** *Sucnr1* deficiency completely reversed apoptosis of MLE-12 induced by succinate-induced polarized AMs (*n* = 3). Data are expressed as mean ± SEM, $^{***}P < 0.001$, vs. WT mice PBS-treated group; $^{###}P < 0.001$, vs. WT mice succinate-treated group. **(E)** *Sucnr1* deficiency suppressed succinate-induced cell apoptosis in the lungs during intestinal I/R. TUNEL-positive cells are represented by red spots with DAPI-stained blue background (*n* = 3). Data are expressed as mean ± SEM. $^{**}P < 0.01$, $^{***}P < 0.001$, vs.WT mice I/R group; $^{###}P < 0.001$, vs. WT mice with succinate+I/R group.
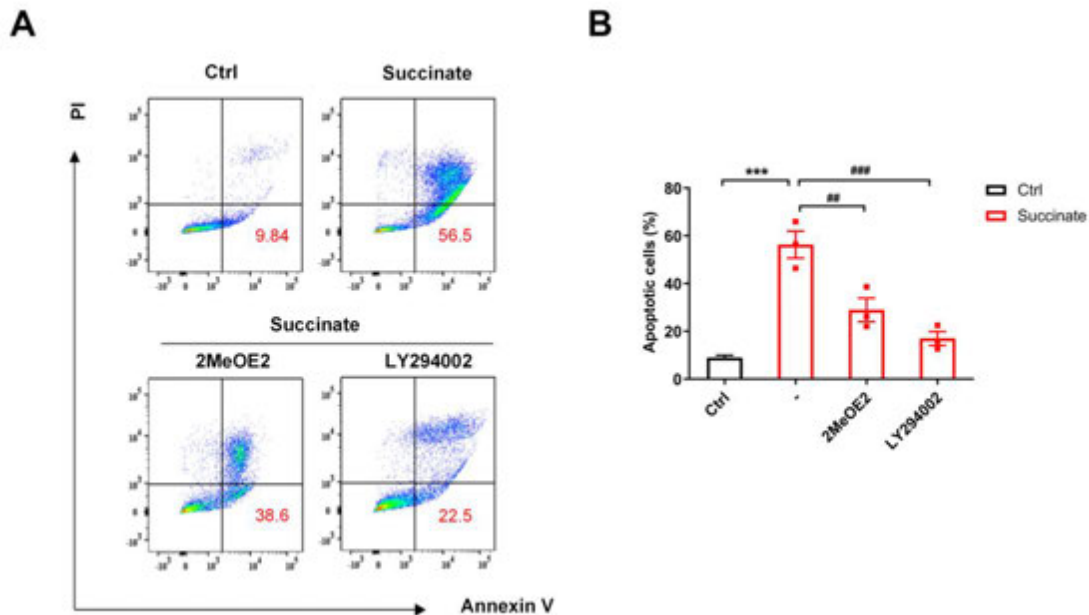
Figure S7: PI3K/AKT/HIF-1α pathway mediated succinate-induced apoptosis of alveolar epithelial cells. (A) Representative images of apoptosis assay results obtained by flow cytometry. **(B)** The succinate-induced increase in apoptosis of MLE-12 cells was suppressed upon pretreatment with 2MeOE2 (100 µmol/L) and LY294002 (10 µmol/L) (*n* = 3). Data are expressed as mean ± SEM. ***P < 0.001, vs. PBS group; ##P < 0.01, ###P < 0.001, vs. succinate-treated group.
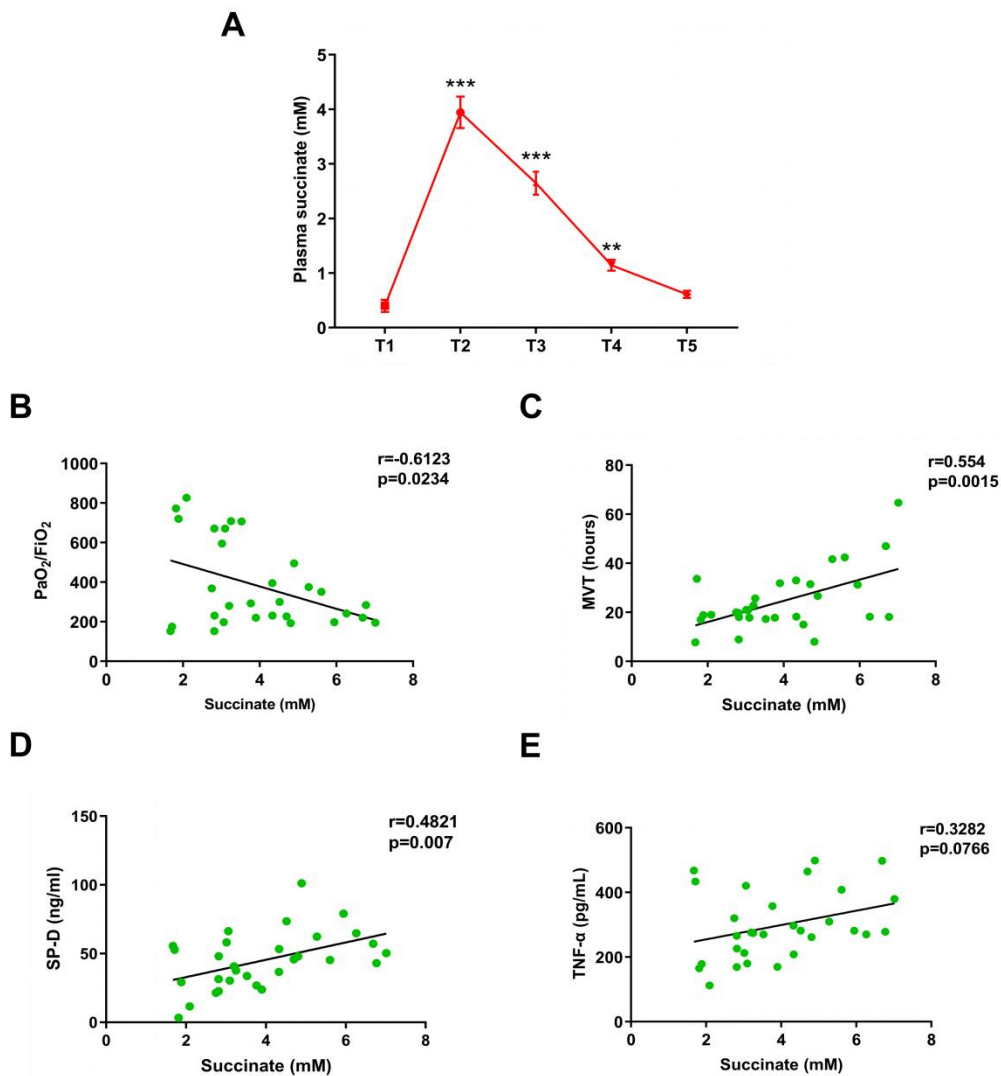
Figure S8. Plasma succinate level correlated with lung injury in cardiac surgical patients after cardiopulmonary bypass (CPB). (A) The levels of plasma succinate were generally increased in patients after CPB surgery. T1, 1 day before surgery or before anesthesia induction; T2, 1 h after surgery; T3, 6 h after surgery; T4, 12 h after surgery; T5, 24 h after surgery. **(B-E)** Correlation between plasma succinate and oxygenation index (PaO_2/FiO_2) (B), mechanical ventilation time (MVT) (C), and surfactant protein-D (SP-D) (D) and TNF-α (E) levels in surgical patients (Spearman's rank correlation). (n = 30). Data are expressed as mean ± SEM, [**]P < 0.01, [***]P < 0.001, vs. T1 group.